universität wien

DIPLOMARBEIT / DIPLOMA THESIS

Titel der Diplomarbeit / Title of the Diploma Thesis

"Metabolic regulation of mitochondrial pathways in oxidative stress"

verfasst von / submitted by

Magdalena Latka

angestrebter akademischer Grad / in partial fulfilment of the requirements for the degree of

Magistra der Pharmazie (Mag.pharm.)

Wien, 2020 / Vienna, 2020

Studienkennzahl lt. Studienblatt / degree programme code as it appears on the student record sheet:	A 449
Studienrichtung lt. Studienblatt / degree programme as it appears on the student record sheet:	Diplomstudium Pharmazie
Betreut von / Supervisor:	Prof. Dr. Carsten Culmsee

This work is dedicated to my family, whose love, patience and trust created a save haven for me while working on this project.

Acknowledgments

Foremost, I would like to express my deepest appreciation to my advisor Prof. Dr. Carsten Culmsee for the facilitation and supervision of this thesis at the Biochemical Pharmacological Center of the Phillips-Universität Marburg. For all the advice and guidance I received I will always be thankful.
I wish to thank my fellow labmates – especially my project mentor Malena Rabenau – for sharing their experience with me. I must also thank the laboratory technician Katharina Elsässer for her practical advice. It was great sharing laboratory with all of you!
I'm deeply indebted to Artur Svidrytski, whose invaluable contribution – to the graphs, to problem solving and to upholding my hopes – cannot be overestimated.
Special thanks to Cagin Tüzün, who has always been there for me during my studying time in Vienna and beyond, and whose extensive knowledge gave me invalueable insights into science.
Last but not least, I would like to thank my family for their unlimited love and unwavering support during my entire life.

Abstract

Background: Bearing in mind that our population is aging and that aging is the most important risk factor for neurodegeneration, there is an urgent need for achieving a better understanding how nerve cells die and how this can be prevented. There is emerging evidence that prior to detectable neurodegeneration neurons struggle with dysregulated metabolism and bioenergetic crises. Mitochondria play a dual role as main energy suppliers for the high energy demanding neurons as well as judges over life and death. Mitochondria with impaired dynamics and acquired electron transport chain defects drive the aging and neurodegenerative processes via energy deprivation, excessive formation of reactive oxygen species (ROS) and activation of cell death pathways. The endogenous strategy to decrease the ROS burden for mitochondria are uncoupling proteins, that dissipate the proton gradient used for ATP synthesis in order to minimize ROS emission from the electron transport chain. Thus, sustaining mitochondrial structure and function represents a gateway to neuroprotection. The pharmacological reduction of the efficiency of energy conversion, e.g. by inhibition of respiratory chain complex I and by shifting glucose utilization from oxidative phosphorylation to glycolysis in order to decrease the oxidative burden for the mitochondria has been shown to be a protective strategy under increased oxidative stress conditions. Such a mild threat to the cells' survival renders cells and animals resilient towards a greater and otherwise fatal stressor via activation of several evolutionary conserved prosurvival pathways, a strategy also known under terms like preconditioning and hormesis. In order to confirm or disprove these paradoxical observations, in this thesis respiratory chain complex I inhibitor phenformin was tested as a neuroprotective agent against oxytosis in HT22 cells. Oxytosis is a form of regulated necrosis, occuring in an ischemic, haemorrhagic and degenerative environment when the antioxidant capacity of the cell is overwhelmed, and is susceptible to changes of lipid, glutamine and iron metabolism, among others.

Methods: For the experiments the murine immortalized neuron-like HT22 cell line was used. Effects of phenformin on metabolic activity and cell viability were measured with the MTT assay. Proliferation rate and cell viability was analysed via real-time impedance measurement with the xCELLigence System. Flow cytometric analyses included the measurement of lipid peroxides with BODIPY, mitochondrial superoxide with MitoSOX, mitochondrial membrane potential ($\Delta\Psi m$) with TMRE and apoptosis/necrosis with Annexin V-FITC/PI fluorescent dyes.

Results: Phenformin showed transient protection against glutamate-induced damage in the flow cytometric analyses of lipid peroxidation, mitochondrial superoxide and apoptosis and in the MTT and xCELLigence experiments. A pretreatment with phenformin before glutamate exposure lead to longer-lasting protective effects, as survival of neurons was maintained through at least 22 h of exposure to glutamate compared to around 12 h in cotreatment mode, indicating expanded protective mechanisms with longer incubation time. Furthermore, the inhibiting effects of phenformin on metabolic activity as well as on proliferation were observed to go hand in hand with protective effects. The mild lowering effect on mitochondrial membrane potential and slight increase of mitochondrial superoxide levels also correlated with increased cell viability.

Conclusions: Phenformin treatment rendered HT22 cells more resistant against oxidative glutamate toxicity. The effects on mitochondrial membrane potential and on mitochondrial superoxide levels indicate direct action of phenformin on mitochondria. Taking into consideration the body of research on other mitochondria-targeted oxytosis-preventing agents, one might attribute the protection rendered by phenformin to complex I inhibition, among other possible mechanisms of action.

Keywords: oxytosis, ferroptosis, phenformin, neuroprotection, mitochondria, complex I inhibition, mitochondrial membrane potential

Zusammenfassung

Hintergrund: Angesichts der Tatsache, dass unsere Bevölkerung altert und das Altern der wichtigste Risikofaktor für Neurodegeneration ist, ist es dringend erforderlich, ein besseres Verständnis dafür zu erlangen, wie Nervenzellen sterben und wie dies verhindert werden kann. Es gibt Hinweise darauf, dass Neuronen vor einer nachweisbaren Neurodegeneration mit einem gestörten Stoffwechsel und bioenergetischen Krisen zu kämpfen haben. Mitochondrien spielen eine doppelte Rolle als Hauptenergielieferanten für die energieaufwändigen Neuronen sowie als Richter über Leben und Tod. Mitochondrien mit beeinträchtigter Dynamik und Defekten der Elektronentransportkette treiben die Alterungs- und neurodegenerativen Prozesse über Energieentzug, übermäßige reaktive Sauerstoffspezies (ROS)-Bildung und Aktivierung von Zelltodpfaden an. Die endogene Strategie zur Verringerung der ROS-Belastung für Mitochondrien sind Entkopplungsproteine, die den für die ATP-Synthese verwendeten Protonengradienten zerstreuen, um die ROS-Emission aus der Elektronentransportkette zu minimieren. Die Aufrechterhaltung der mitochondrialen Struktur und Funktion stellt somit ein Tor zur Neuroprotektion dar. Es ist bekannt, dass die pharmakologische Verringerung der Effizienz der Energieumwandlung, z.B über die Hemmung des Atmungskettenkomplexes I und die Verlagerung der Glukoseverwertung von der oxidativen Phosphorylierung zur Glykolyse zur Verringerung der oxidativen Belastung der Mitochondrien führt und eine Schutzstrategie unter Bedingungen mit erhöhtem oxidativen Stress darstellt. Solch eine milde Bedrohung des Überlebens der Zellen macht Zellen und Tiere durch die Aktivierung mehrerer evolutionär konservierter Prosurvival-Pfade gegenüber einem größeren und ansonsten tödlich verlaufenden Stressor widerstandsfähig. Diese Strategie ist auch unter Begriffen wie Vorkonditionierung und Hormese bekannt. Um diese paradoxen Beobachtungen zu bestätigen oder zu widerlegen, wurde in dieser Arbeit der Atmungskettenkomplex I-Inhibitor Phenformin als neuroprotektiver Wirkstoff gegen Oxytose in HT22-Zellen getestet. Oxytose ist eine Form der regulierten Nekrose, die u.a. im ischämischen, hämorrhagischen und degenerativen Milieu auftritt, wenn die antioxidative Kapazität der Zelle überfordert ist und die durch viele metabolische Prozesse, wie z.B. Veränderungen des Lipid- und Glutaminstoffwechsels sowie der Eisenhomöostase manipulierbar ist.

Methoden: Für die Experimente wurde die murine immortalisierte neuronähnliche HT22-Zelllinie verwendet. Die Auswirkungen von Phenformin auf die Stoffwechselaktivität und die Lebensfähigkeit der Zellen wurden mit dem MTT-Assay gemessen. Die Prolifer-

ationsrate und die Lebensfähigkeit der Zellen wurden mittels Echtzeit-Impedanzmessung mit dem xCELLigence-System analysiert. Durchflusszytometrische Analysen umfassten die Messung von Lipidperoxiden mit BODIPY, Mitochondrien-Superoxid mit MitoSOX, mitochondrialem Membranpotential ($\Delta\Psi$m) mit TMRE und Apoptose/Nekrose mit Annexin V-FITC/PI-Fluoreszenzfarben.

Resultate: Phenformin zeigte in den durchflusszytometrischen Analysen der Lipidperoxidation, des mitochondrialen Superoxids und der Apoptose sowie in den MTT- und xCELLigence-Experimenten einen vorübergehenden Schutz gegen Glutamat-induzierte Schäden. Eine Vorbehandlung mit Phenformin vor der Exposition mit Glutamat führte zu länger anhaltenden Schutzeffekten, da das Überleben der Neurone über mindestens 22 Stunden im Vergleich zu etwa 12 Stunden im Cotreatment-Modus aufrechterhalten wurde, was auf erweiterte Schutzmechanismen durch längere Inkubationszeit hinweist. Weiterhin wurde beobachtet, dass die Hemmwirkung von Phenformin auf die Stoffwechselaktivität sowie auf die Proliferation mit schützenden Wirkungen einhergeht. Die leichte Erniedrigung des mitochondrialen Membranpotentials und der leichte Anstieg der mitochondrialen Superoxidspiegel korrelierten ebenfalls mit einer erhöhten Lebensfähigkeit der Zellen.

Schlussfolgerungen: Durch die Behandlung mit Phenformin wurden HT22-Zellen resistenter gegen oxidative Glutamat-Toxizität. Die Auswirkungen auf das mitochondriale Membranpotential und die mitochondrialen Superoxidspiegel deuten auf eine direkte Wirkung von Phenformin auf Mitochondrien hin. Unter Berücksichtigung der zahlreichen Forschungsarbeiten zu anderen auf Mitochondrien gezielten, Oxytose verhindernden Wirkstoffen könnte man den durch Phenformin bewirkten Schutz neben anderen möglichen Wirkungsmechanismen auch der Komplex-I-Hemmung zuschreiben.

Schlüsselwörter: Oxytose, Ferroptose, Phenformin, Neuroprotektion, Mitochondrien, Komplex I-Hemmung, mitochondriales Membranpotential

Abbreviations

12/15-LOX 12/15-lipoxygenase
AIF apoptosis-inducing factor
AMPK AMP-activated protein kinase
ATP adenosine triphosphate
AV/PI Annexin V-FITC/Propidium Iodide
Bid BH3-interacting domain
cGMP cyclic guanosine monophosphate
CI-V complex I-V
CR caloric restriction
DMEM Dulbecco's modified Eagle's medium
DMSO dimethyl sulfoxide
DNA deoxyribonucleic acid
ER endoplasmic reticulum
ETC electrone transport chain
FACS fluorescence-activated cell scanning
FCS fetal calf serum
FITC fluorescein isothiocyanate
FMN flavin mononucleotide
GPX4 glutathione peroxidase 4
GSH glutathione
H_2O_2 hydrogen peroxide
HT22R glutamate-resistant HT22 cells
MMP, $\Delta\Psi m$ mitochondrial membrane potential
MPT mitochondrial permeability transition
mPTP mitochondrial permeability transition pore
mROS mitochondrial reactive oxygen species
mTORC1 mechanistic target of rapamycin complex 1
MTT 3-(4,5-Dimethylthiazolyl-2)-2,5-diphenyl tetrazolium bromide
NAD(P)H nicotinamide adenine dinucleotide (phosphate)
NCI normalized cell index
ND neurodegenerative disease
OMM outer mitochondrial membrane

PBS phosphate buffered saline

PUFA-PLs phospholipids transesterified with polyunsaturated fatty acids

RCD regulated cell death

RET reverse electron transport

ROS reactive oxygen species

TCA tricarboxylic acid cycle

TE trypsin-EDTA

TMRE tetramethylrhodamine ethyl ester

UCP uncoupling protein

Contents

Chapter 1

Introduction

1.1 Neuronal cell death in aging and neurodegeneration

There are many ways a neuron can die, or better – many biochemically linked catabolic events that lead to cell processing. Apoptosis and necrosis are viewed as opposite extremes in a spectrum of cell death with apoptosis being one of the many regulated cell death (RCD) pathways, while unregulated necrosis is the only unprogrammed form of cell demise. Other regulated cell death routines, which have been described by several research teams at least in some cells and tissues during neurodegeneration, include oxytosis (ferroptosis), parthanatos, pyroptosis, necroptosis, lysosomal membrane permeability, MPT-driven necrosis, endoplasmic reticulum (ER)-stress mediated apoptosis, just to name a few [1, 2] (Fig. 1.1). Sometimes the unfinished cell death execution by an abrupted cell death pathway is being continued by another cell death pathway [3]. Extensive research is still trying to elucidate the relative contributions of the various death mechanisms to neurodegeneration in order to increase therapeutic efficacy. The death pathways seem to depend on the neuronal population, its age, stage of dysfunction, and the nature and extent of the death-inducing insult. Mitochondria play a critical gatekeeper role in determining cellular fate [4, 5]. Integration of pro- and antiapoptotic signals by the network of Bcl-2 family proteins determines whether or not the outer mitochondrial membrane (OMM) is permeabilized and multiple mitochondrial death-promoting factors liberated into the cytosol [6–8].

Although neurodegenerative diseases (NDs) are a heterogeneous group of disorders with characteristic pathophysiology and selective neuroanatomical distributions that affect vulnerable neuronal populations due to their unique molecular and morphological characteristics, the neurological symptoms are the result of either neuronal dysfunction or death [9]. The biggest risk factor for neurodegeneration is an aberrant aging process, in which case it is called sporadic in nature [10, 11]. The most prevalent NDs are proteinopathies. These misfolded proteins have aberrant interactions with themselves and other biomolecules that result in aggregates, mitochondrial dysfunction and oxidative

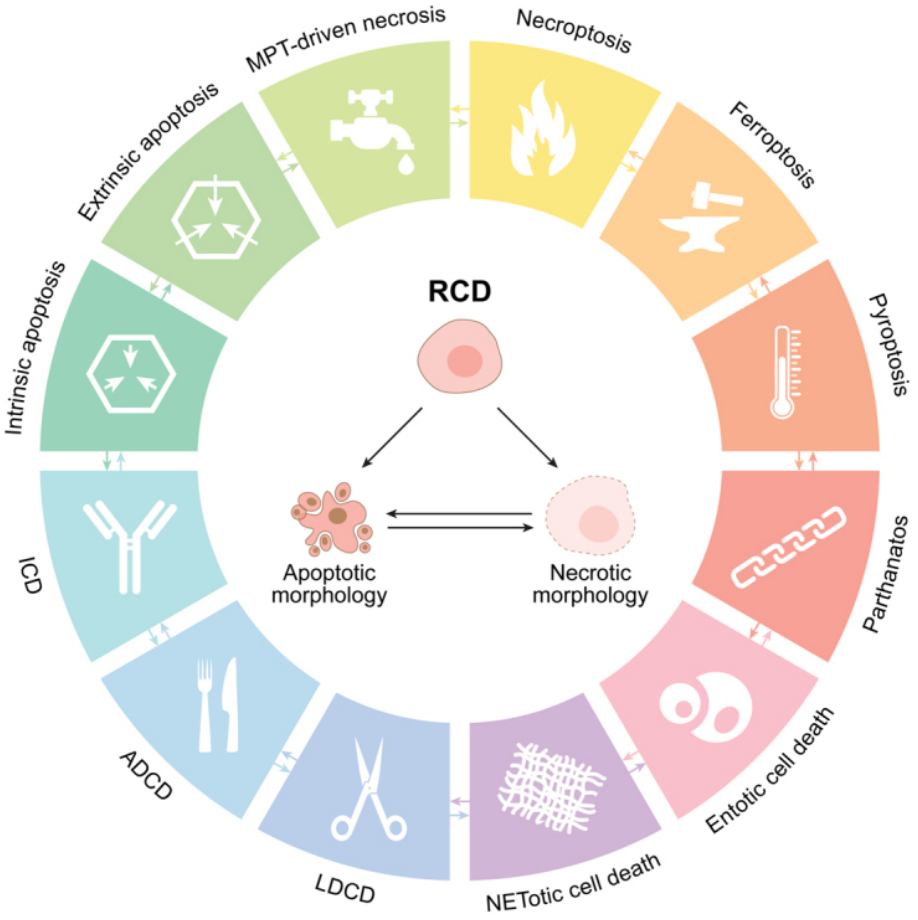

Figure 1.1: Major regulated cell death (RCD) pathways.
Mammalian cells dispose of a plethora of cell death pathways with a high degree of interconnectivity. Each type of RCD can exhibit morphological features ranging from fully necrotic to fully apoptotic. ADCD: autophagy-dependent cell death, ICD: immunogenic cell death, LDCD: lysosome-dependent cell death, MPT: mitochondrial permeability transition [1].

stress [12,13]. The clinical symptoms usually become evident during an advanced state of disease, when the death of neurons cannot be compensated anymore by the remaining neurons [14]. There are certain processes during aging – reviewed as hallmarks of brain aging by Mattson et al. (2018) – that render the aging brain vulnerable to neurodegeneration and decreases the ability to mount a successful stress response during stroke. These include e.g. mitochondrial dysfunction; the intracellular accumulation of oxidatively damaged proteins, nucleic acids, and lipids; impaired cellular "waste disposal" mechanisms (autophagolysosome and proteasome functionality); impaired adaptive stress response signalling; compromised DNA repair; dysregulated neuronal Ca^{2+} handling and inflammation. None of these hallmarks occurs in isolation as they are intertwined, highly interdependent pathways [15]. The bioenergetic hypothesis puts dysregulated energy metabolism at the root of the aging process and advocates for sequential events originating from dysregulated nutrient sensing and metabolic deficits to propagation of neuronal dysfunction and to neurodegeneration [15, 16].

1.2 Mechanism of oxytosis and HT22 cells as a model system

Glutamate is the most abundant excitatory neurotransmitter in the central nervous system and its extracellular concentration is a critical determinant of neuronal cell fate [17]. In the case of brain trauma, ischemia, epilepsy and NDs, extracellular glutamate may reach millimolar concentrations and induce damage through receptor-mediated excitotoxicity [18] and through oxidative glutamate toxicity (syn. oxytosis) [19, 20] (Fig. 1.2), two cell death pathways, which are integrated in parallel and occur both in neurons and oligodendrocytes [21,22]. Oxytosis has been extensively studied in the neuron-like HT22 cell line, primary neuronal cultures and oligodendrocytes. HT22 cells are immortalized, transformed mouse hippocampal cells, which express no functional ionotropic glutamate receptors and are therefore not susceptible to excitotoxicity. A high extracellular glutamate concentration inhibits the cystine/glutamate antiporter system x_c^- (xCT), so cystine, which is needed for the synthesis of the antioxidant glutathione (GSH), cannot enter the cell due to the unfavourable concentration gradient. GSH is the cofactor for the selenoprotein glutathione peroxidase 4 (GPX4), the major detoxifier of peroxidized lipids (L-OOH) in membranes [23, 24]. Therefore, this cell line is a model for monitoring neuronal responses to oxidative stress and tool to screen for agents protective against iron-dependent lipid peroxidation, Ca^{2+} overload and disturbed mitochondrial dynamics.

In oxytosis, the accumulation of ROS is biphasic, with the imbalance between the constitutive synthesis of ROS by autophagy or lysosomal activity and their detoxification by GPX4 causing the first and mitochondrial dysfunction causing the second, more pronounced burst of ROS [20, 25]. A key factor involved in oxytosis execution is acyl-CoA synthetase long-chain family member 4 (ACSL4), which catalyzes esterification of arachidonoyl and adrenoyl acyls into phosphatidylethanolamines [26], whereafter lysophosphatidylcholine acyltransferase (LPCAT3) catalyzes their insertion into membrane phospholipids [27]. These polyunsaturated-fatty-acid-containing phospholipids (PUFA-PLs) are the most vulnerable lipid species due to the presence of bis-allylic sites. They are either enzymatically or nonenzymatically converted into lipid hydroperoxides by PEBP1/15-LOX complexes or other iron-containing lipoxygenases (LOXs) [27–30] or they can be oxidized by Fe^{3+}, which yields highly reactive alkoxy radicals (L-O• radical) and free radical-mediated chain reactions. A unique characteristic of 12/15-LOX of the brain is that its enzymatic activity is induced by highly diminished GSH levels and increased ROS [31–33], which is approximately after 6 hours of glutamate exposure. Its metabolites, 12- and 15- hydroxyeicosatetraenoic acids (12-/15-HETE) directly damage mitochondria [34], they are also activators of soluble guanylate cyclases, which increase the concentration of intracellular cyclic guanosine monophosphate (cGMP) thereby causing a dysregulated influx of Ca^{2+} through cGMP-dependent Ca^{2+} channels and also through store-operated Ca^{2+} entry (SOCE) member ORAI1 [35]. However, the elevation of intra-

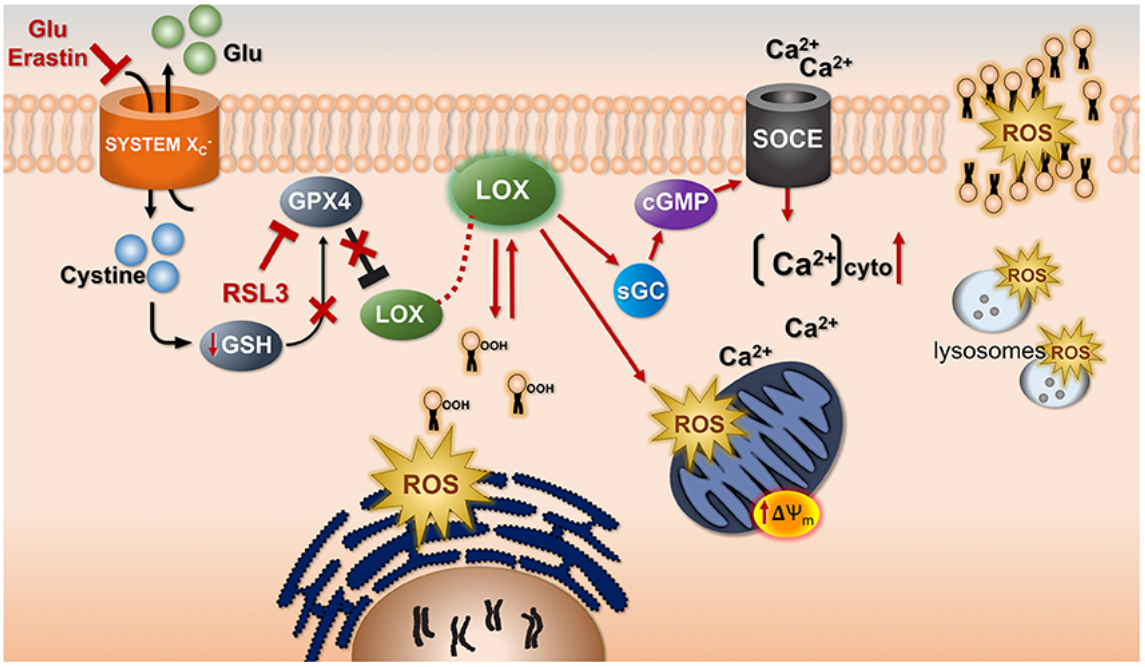

Figure 1.2: Oxytosis (Ferroptosis).
Glutamate (Glu) and erastin inhibit the cystine transport into the cell through system x_c^-, which leads to decreased synthesis of the antioxidant glutathione (GSH) and inactivation of the GSH-dependent enzyme GPX4. RSL3 directly inhibits GPX4. Subsequent activation of lipoxygenase (LOX) accelerates the formation of lipid hydroperoxides (lipid icons with OOH) in membranes. LOX metabolites like cGMP open calcium channels. There is an interplay between reactive oxygen species (ROS) and Ca^{2+}. SOCE: store-operated Ca^{2+} entry [58].

cellular Ca^{2+} cannot be completely attributed to its influx from the extracellular space but is also dependent on organelles such as mitochondria and the ER [36, 37]. High cytosolic Ca^{2+} increases 12/15-LOX membrane binding and enzyme activity resulting in a vicious cycle [32, 38].

A hallmark of oxytosis is the loss of mitochondrial form and function. Oxytosis is associated with mitochondrial Ca^{2+} overload, an upregulation and oligomerization of VDAC1 [39], mitochondrial hyperpolarization, enhanced oxygen consumption uncoupled of adenosine triphosphate (ATP) production [40] and increased mitochondrial ROS production, supposedly from a flavin mononucleotide (FMN) group within respiratory complex I (CI) [20]. 8-10 h after induction of glutamate toxicity, Bid and Drp1 translocate to the mitochondria and cause a sequence of events leading to structural changes, which morphologically characterize oxytosis, like loss of cristae, diminished mitochondrial membrane densities, rupture of the outer mitochondrial membrane (OMM), fission and perinuclear accumulation so that apoptosis-inducing factor (AIF) can diffuse to the nucleus with a short trajectory leading to nuclear chromatin condensation and large molecular weight DNA fragmentation and cell death within only a few minutes after release [41–43]. Of note, this form of cell death was recently defined as ferroptosis. The literature might make them appear distinct, since some characteristics have been studied in more detail under the name of either oxytosis (the role of cGMP, LOX and Ca^{2+} mostly in HT22 cells, which is

why it is known as a calcium-dependent form of RCD) or ferroptosis (the iron-dependent generation of detrimental lipid peroxides mostly in cancer cells and fibroblasts), but the core process of lipid peroxide accumulation, the involvement of GSH and GPX4 and the iron-dependency is common to both mechanisms. Obviously, tissue-specific variations exist [44]. The sensitivity to oxytosis is regulated by the metabolism of amino acids (glutaminolysis [45]), iron [45,46], lipids [47] and mevalonate (specifically, the production of coenzyme Q_{10}) [48, 49] and NADPH [50]. Compounds acting directly on mitochondria and causing metabolic constraints, like the uncoupler FCCP [51], inhibitors of the electrone transport chain (ETC) rotenone [52] and antimycin A, flavin-protein binding agents like diphenyliodonium (DPI) and clorgyline [53], or mitochondrial Ca^{2+} regulators like the Ca^{2+} uptake inhibitor ruthenium red [51], and activators of small conductance Ca^{2+} -activated K^{+} (SK) channels, that reduce mitochondrial respiration and restore mitochondrial Ca^{2+} homeostasis [54, 55], have shown to prevent oxytosis. The tricarboxylic acid (TCA) cycle has been shown to promote cellular GSH depletion in combination with cysteine deprivation leading to oxytosis [56]. Studies on glutamate-resistant HT22 cells (HT22R), generated by repeated exposure to detrimental concentrations of glutamate, revealed that HT22R survive, in part, due to metabolic reprogramming, as they show reduced mitochondrial respiration and increased glutathione recovery through the pentose phosphate pathway. Their mitochondria show seemingly contradictory features like increased mitochondrial Ca^{2+} and superoxide, reverse activity of the ATP synthase leading to outward protone pumping while hydrolyzing ATP – all measures needed to maintain or even elevate the mitochondrial membrane potential ($\Delta\Psi$m) [57].

1.3 Bioenergetic challenge-based neuroprotection: biguanides

Biguanides are drugs with indirect pleiotropy on core metabolic hallmarks of aging [16, 59, 60]. Metformin is currently the first-line therapy for type 2 diabetes (T2D) with well-established anti-hyperglycemic and insulin-sensitizing action and a high safety profile [61]. The worldwide long-term clinical use and the plethora of mechanistic studies on it have evidenced surprising and beneficial side effects beyond diabetes management, including cardioprotection [62], renoprotection [63], obesity [64], polycystic ovary syndrom (PCOS) [65], preeclampsia [66], nonalcoholic fatty liver disease (NAFLD) [67, 68], atherosclerosis [69], rheumatoid arthritis [70], cancer [71–73], mood disorders [74] and neurodegeneration [75], however there is currently not sufficient clinical evidence that supports all these new applications. Many of the clinical outcomes can be traced back to the anti-inflammatory [76, 77], ER- and oxidative stress-attenuating effects [78, 79] as well as the alteration of cellular bioenergetics, nutrient sensing and utilization [80, 81]. The diverse effects of metformin are the result of the interaction with numerous enzymes,

including respiratory complex I [82–84], AMP-activated protein kinase (AMPK) [85] and mTORC1 [86]. AMPK is a fundamental component of cellular responses to stresses that threaten cell viability in times of intracellular energy starvation by means of phosphorylation of over 1000 targets, which shuts off energy consuming processes like protein translation, lipogenesis and gluconeogenesis and turns on energy conserving pathways like autophagy and mitochondrial beta-oxidation of fatty acids [87–93]. It also works as a key regulator of mitochondrial biogenesis [94, 95]. mTORC1 stimulates growth and protein synthesis and short-term activation increases mitochondrial respiration and biogenesis in cultured cells. However, mTORC1 inhibition of autophagy can allow damaged mitochondria to accumulate [96–98]. Inhibition of mTORC1 is consistently associated with extended lifespan in model organisms from yeast to mice [99, 100]. Intriguingly, metformin is considered as one of the most promising anti-aging drugs, that could potentially slow down aging and extend lifespan, as observed in some model organisms [101, 102].
Phenformin was withdrawn from the markets in most countries due to a much higher incidence of lactic acidosis. For comparison, the frequency of lactic acidosis for metformin is 0–9 cases, for phenformin 40–64 cases for 100,000 person-years, however, those are mostly confined to patients with impaired renal function or polymorphism of drug metabolism [103, 104]. Both biguanides have similar applications, in fact, phenformin is believed to be essentially a more lipophilic, stronger version of metformin [105, 106], presumably because it is transported with a greater affinity and kinetics into cells [107, 108], because of stronger interactions with CI leading to 10 times more potent CI inhibition [82, 109] or because of metformin's self-limiting entry into the mitochondria [83, 110]. It is also known that metformin, the lipophilic biguanides phenformin and buformin and diguanides each modulate mitochondrial oxidation of CI substrates by distinct mechanisms [105, 109, 111–113]. Depending on the binding site, ROS formation can either rise or fall [114]. Metformin is believed to cause a mitohormetic response to ROS [115]. In the long run, metformin decreases ROS levels, supposedly due to inhibition of reverse electron transport (RET) between complex II and complex I [116, 117] (see Fig. 1.3).

Phenformin has been shown to both incite an mROS signal [118] and to decrease superoxide formation at CI [119]. CI (syn. NADH:ubiquinone oxidoreductase) is the sole entry point for reduced NADH from the tricarboxylic acid cycle (TCA) into the ETC [120]. The diminished flow of electrons throughout the ETC and diminished proton gradient ultimately lead to diminished ATP production at complex V (ATP synthase). This results in a compensatory increase in glycolysis. However, if the compensatory activation of glycolysis cannot meet the cellular ATP requirements and the AMP/ATP ratio rises, AMPK becomes activated [121]. Although the positively charged biguanides accumulate a thousand-fold in the mitochondrial matrix following the negative $\Delta\Psi m$, some researchers question CI inhibition as an in-vivo mechanism of action of metformin due to the supraphysiological concentrations needed for CI inhibition in vitro. However, there is more than one molecular explanation for what happens downstream of CI inhibition.

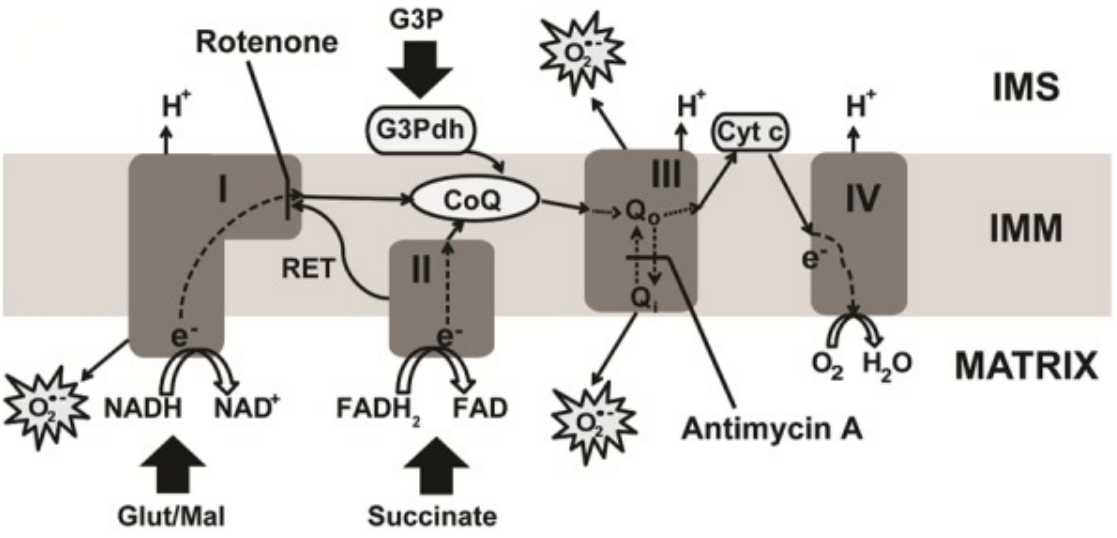

Figure 1.3: Respiratory chain organization, mitochondrial substrate metabolism, electron leakage sites, and effects of respiratory modulators.
The ETC consists of four multimeric complexes I-IV. Electrons from NADH or $FADH_2$ enter the chain via CI or CII, respectively. The horizontal electron transport is coupled to a vectorial proton transport across the membrane at complexes I, III and IV. The proton gradient is used for ATP synthesis. The most important cellular ROS sources are CI and CIII. Between CII and CI reverse electron transport (RET) can occur. Rotenone is a CI inhibitor. Metformin is supposedly also an inhibitor of glycerol-3-phosphate-dehydrogenase (G3Pdh). Glut/Mal: glutamate/malate, G3P: glycerol-3-phosphate, CoQ: Coenzym Q, IMS: intermembrane space, IMM: inner mitochondrial membrane [133].

Namely, at therapeutically-relevant concentrations metformin acts via the inhibition of the lysosomal vATPase which promotes formation of the AXIN-LKB1-vATPase complex on the lysosomal surface and allosterically activates AMPK proteins while simultaneously inhibiting the mTORC1 complex anchored on the lysosomal surface [122, 123]. There are indications that phenformin activates AMPK through a different mechanism [124]. The end result of biguanide exposure is cellular energetic stress with a shift towards a caloric restriction (CR)-like gene expression profile [125]. Metformin has shown additional in vitro effects on mitochondria, like the inhibition of dynamin-related protein 1 (Drp1)-mediated mitochondrial fission [69] or the inhibition of mitochondrial permeability transition pore (mPTP) opening [126–128]. Less researched mechanisms of metformin action include its in-vitro interactions with copper [111, 129].

Studies of phenformin in neuronal cells are scarce. Antioxidative effects were observed [130]. Decades ago, its effects on mitochondrial Ca^{2+} levels were investigated. In one study, administration of phenformin to rats and guinea-pigs resulted in decreased mitochondrial Ca^{2+} [131]. Intriguingly, phenformin was found to interfere with NMDA-receptor subunit constellation thus decreasing glutamate-induced Ca^{2+} influx and rendering hippocampal cells more resistant against excitotoxicity [132].

1.4 Aim of the thesis

The questions that urgently need answers in an aging population are why and how a neuron dies as a result of different stimuli, and more importantly – how is it protected from death in some circumstances, what are the signals that trigger the initiation of the recovery process of anastasis, how is cellular damage repaired and with what physiological or pathological implications. Ultimately, it will be of importance to provide strategies for transferring this knowledge from research to clinical practice. The aim of this thesis was to test the neuroprotective effects of phenformin in the HT22 cell model system. The change in bioenergetics incited by phenformin was tested against an oxidative stress insult induced by glutamate. A particular focus lied on changes of mitochondrial parameters induced by oxidative stress and by the protective agent. The hypothesis was that if phenformin could reduce the oxidative burden for the mitochondria and thus prevent mitochondrial destabilisation, then the neurons would survive the oxidative stress challenge.

Chapter 2

Materials and Methods

2.1 Chemicals and reagents

All standard chemicals commercially available were obtained from Sigma-Aldrich (Taufkirchen, Germany) or Roth (Karlsruhe, Germany), if not declared otherwise. Ultrapure, demineralized water for aseptic preparation of solutions and for media used in the cell culture was generated by the SG Ultra Clear UV plus pure water system (VWR, Darmstadt, Germany) and sterilized either using a steam autoclave (Systec V-40, Systec GmbH, Wettenberg, Germany) or by filtration using 0.22 µM filter sets (Sarstedt, Nümbrecht, Germany). Following kits were used in this work according to the manufacturer's protocol (table 2.1). Changes in the protocol are described in the corresponding sections. Phenformin (N-Phenethylbiguanide) (Fig. 2.1) and metformin (1,1-Dimethylbiguanide) (Fig. 2.2) (Sigma-Aldrich, Taufkirchen, Germany) were dissolved in sterilized water to a concentration of 100 mM and 1 M, respectively. The stock solutions were portioned for single-time usage to avoid freeze-thawing cycles, stored at $-20\,^{\circ}\mathrm{C}$ and diluted with medium prior to each experiment up to the final concentrations. New stock solutions were prepared approximately once a month.

Table 2.1: Kits

Kit	**Company**
Annexin-V-FITC Detection Kit	Promokine, Heidelberg, Germany
Bodipy (581/591 C11)	Thermo Fisher Scientific, Darmstadt, Germany
MitoSOX^{TM}	Thermo Fisher Scientific, Darmstadt, Germany
MitoPT^{TM} TMRE	ImmunoChemistry Technologies, Bloomington, USA

2.1.1 Inducers of cell death

The 1 M stock solution of glutamate was prepared by dissolving L-glutamic acid monosodium salt hydrate (Sigma-Aldrich, Taufkirchen, Germany) in Dulbecco's modified

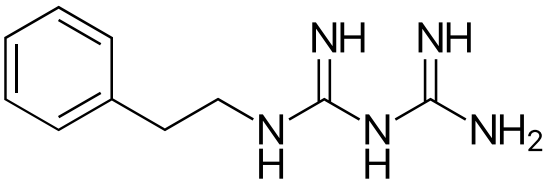

Figure 2.1: Phenformin

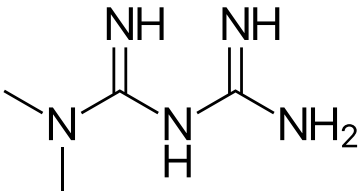

Figure 2.2: Metformin

Eagle's medium (DMEM; Sigma-Aldrich, Taufkirchen, Germany). The pH of the stock solution was adjusted to 7.2 with concentrated sodium hydroxide solution (NaOH) and stored at $-20\,^{\circ}\mathrm{C}$. For cell death induction, the stock solution was diluted in DMEM for a final concentration of usually 8 mM. The 10 mM stock solution of erastin in dimethyl sulfoxide (DMSO) (Calbiochem, Darmstadt, Germany) was stored at $-20\,^{\circ}\mathrm{C}$ and diluted with DMEM to a concentration of 1 µM for cell death induction.

2.1.2 Inhibitors of cell death

The BID-inhibitor BI-6c9 (Sigma-Aldrich, Taufkirchen, Germany) was used as a positive control for protection against cell death. The 10 mM stock solution of BI-6c9 in DMSO was stored at $-20\,^{\circ}\mathrm{C}$. For BID inhibition it was diluted in DMEM to a final concentration of 10 µM.

2.2 Cell culture materials

All sterile plastic ware used in this work is listed in table 2.2. The xCELLigence Real-Time Cell Analysis (RTCA) and the E-plates for the impedance measurements were obtained from Roche Diagnostics, Mannheim, Germany.

Table 2.2: Plastic commodities

Plastic commodities	**Company**
Company T75 flasks	Greiner (Frickenhausen, Germany)
24-well plates	Greiner (Frickenhausen, Germany)
96-well plates	Greiner (Frickenhausen, Germany)
96-well E-plates	Roche (Mannheim, Germany)
0.2 mL, 1.5 mL, 2 mL Eppendorf tubes	Sarstedt (Nümbrecht, Germany)

Table 2.3: Culture medium for HT22 cells

Substance	Volume
fetal calf serum (FCS)	50 mL
Penicillin (100 U/mL), Streptomycin (100 µg/mL)	5 mL
L-glutamine 2 mM	5 mL
DMEM with 4.5 g/L glucose and 110 mg/L sodium pyruvate	ad. 500 mL

Table 2.4: Trypsin-EDTA (1x TE)

Substance	Volume
Trypsin (7,500 U/mg)	100 mg
EDTA	40 mg
PBS	ad. 200 mL

2.2.1 Cultivation of HT22 cells

HT22 cells, an immortalized, transformed murine hippocampal cell line used for all experiments, were derived from Gerald Thiel (Homburg/Saar, Germany) with kind permission of David Schubert (Salk Institute, San Diego, US). DMEM with 10% fetal bovine serum (FBS; Biochrom, Berlin, Germany) was prepared as described in table 2.3.

All reagents for 1x TE (Trypsin-EDTA) were obtained from Sigma Aldrich (Taufkirchen, Germany) and prepared as shown in table 2.4. All reagents for phosphate buffered saline (PBS) were obtained from Sigma Aldrich (Taufkirchen, Germany) and prepared as shown in table 2.5.

HT22 cells were cultivated in T75 flasks in a humidified incubator with 5% CO_2 at 37 °C and split in a 1:5 ratio for usage after 2 nights or 1:20 ratio for usage after 5 nights. For splitting, growth medium was removed and remainders of it washed away with 5 mL PBS. For cell detachment an appropriate amount (usually 2 mL) of trypsin solution was added and cells were incubated 2–5 min. Trypsin digests the surface proteins used for adherence and the EDTA chelates calcium- and magnesium ions to facilitate the adhesion. The enzymatic activity of trypsin was inhibited by at least 4 times the amount of DMEM. The fetal calf serum contains protease inhibitors that deactivate trypsin. The cell suspension was centrifuged at 1,000 g for 5 min; the supernatant was discarded and the cell pellet was resuspended in 5–10 mL fresh growth medium. To seed cells for experiments, the cell count of the cell suspension was determined by pipetting 10 µL cell suspension into the

Table 2.5: Phosphate buffered saline (PBS), pH 7.4

Substance	Volume
NaCl	9 g
Na_2HPO_4	0.527 g
KH_2PO_4	0.144 g
HCl 0.1 M	q.s. for pH 7.4
Bidest. H_2O	ad. 1 L

counting field of a Neubauer-Zählkammer (Brand, Wertheim, Germany). 3-4 big squares of the Neubauer-Zählkammer were counted to determine the number of cells per 1 ml. Depending on the experimental need the appropriate amount of cell suspension was diluted in DMEM and seeded in the corresponding culture dish.
The total amount of culture medium per well in 96-well plates was 100 µL in the cotreatment experiments and 200 µL in pretreatment experiments, in 24-well plates 500 µL and 1 mL, respectively.
For the MTT assays with a time point of 8–12 h a seeding cell number of 7,500/ well was used, whereas for the 16 h time point it was 6,000/well. For the xCELLigence experiments in cotreatment mode a seeding cell number of 6,000/well was used, for the pretreatment mode 3,000 - 7,500/well depending on planned treatment time after estimating growth rate. For the FACS measurements in cotreatment mode with a 10 or 12 h time point a seeding cell number of 50,000/well was used, for the 16 h time point 40,000/well, in the pretreatment mode 30,000/well.

2.2.2 Treatment procedures

Generally, HT22 cells were cultured until they reached 70–80 % confluency. Growth medium was removed and replaced by medium containing phenformin, metformin, inhibitors or inducers of apoptosis for cotreatment experiments. After a pretreatment with phenformin the medium was not removed, but instead diluted with fresh medium in the ratio 1:2 or with medium with double the needed amount of glutamate. Between 8 h and 44 h later, cells were analyzed following standard procedures for the MTT assay or flow cytometry.

2.3 Cell viability assays

2.3.1 Morphological analysis of cell viability

Morphological changes of HT22 cells indicating cell death were detected via transmission light microscopy using Leica DM IL LED microscope (Leica, Wetzlar, Germany) which was equipped with a Lumenera Infinity 2 digital camera (Lumenera Corporation, Ottawa, Canada). HT22 cells are attaching cells with spindle-shaped morphology. Cell death is characterized by dettachment and a significant decrease in light refraction.

2.3.2 MTT assay

The MTT assay is used as a simple preliminary cell viability assay. It is a spectrophotometrical assay. The watersoluble yellow salt 3-(4,5-dimethylthiazolyl-2)-2,5-diphenyl tetrazolium bromide (MTT, Merck KGaA, Germany)) is reduced to an insoluble purple

formazan mainly by NAD(P)H-dependent oxidoreductases of the cytoplasm, the endoplasmic reticulum and mitochondrial enzymes. Cells with a low metabolism reduce very little MTT. Since this reaction doesn't happen in dead cells, the assay usually correlates with cell viability. The assay was performed in 96-well plates. After treatment, 20 µL MTT-solution (2.5 mg/mL in PBS) per well was added to the culture medium and incubated for 1 h at 37 °C. Formazan formation was stopped by removal of the medium and cell membrane permeabilisation was achieved via ice crystal formation after storage of the plate for at least 1 h at −80 °C. After freezing, 70 µL DMSO per well was added and incubated for 1 h at 37 °C on a shaker to dissolve the formazan. Formazan absorbance was measured spectrophotometrically at 570 nm with FluoStar OPTIMA (BMG Labtech, Ortenberg, Germany), while background signals at 630 nm were substracted. The measured absorbance values were calculated as percentage of the absorbance of untreated control cells, which was set at 100%. Standard deviation was calculated and shown as % in relation to the mean of control cell absorbance.

2.3.3 xCELLigence Real-Time Cell Analysis

The xCELLigence System is a real-time electrical impedance monitoring assay to quantify proliferation, morphology change, attachment quality and cell death kinetics. It is performed in special culture plates named E-plates, which have gold microelectrodes fused to the bottom surface. In the absence of cells electric current flows freely through culture medium from the negative to the positive terminal. The impedance of electron flow is caused by adherent living cells while cell detachment due to cell death leads to higher electron flow through the gold electrodes. Changes of electrode impedance were reported using a unitless parameter called Normalized Cell Index (NCI) as a function of time by RTCA Software 1.2 (Roche Diagnostics, Penzberg, Germany). A background measurement (3 measurements every 5 min) with 100 µL culture medium per well was performed before seeding of cells for calculation of the effects of medium itself on the impedance measurements. Treatment of cells was performed, when a cell index between 0.6 and 1 was reached. Cooling of the E-plate during treatment causes a reduction in electrode impedance visible as a downward spike of the cell index curve. To avoid the spike, the measurement should be restarted after the E-plate warmed up back to the incubation temperature. To prevent the influence of variance of seeding densitiy among and within the groups, the cell index was normalized to 1.0 for all wells at treatment start. After the experiments the E-plates were recycled by trypsinization for at least 30 min in the incubator and washed at least three times with 150 µL bidest.H_2O/well followed by an UV-irradiation for 30 min to restore sterility.

2.4 Flow cytometric measurements

Fluorescence-activated cell sorting (FACS) is a laser-based technology to count and sort cells in a narrow stream of liquid. FACS generates multiple information at the single cell level in a high-throughput manner. When combined with a fluorescent label or fluorochrome, the fluorescence intensity of each cell can be captured while passing the capillary. The interaction of the cells with the laser light beam is measured by an electronic detection apparatus as light scatter and fluorescence intensity.

2.4.1 Sample preparation

For FACS experiments HT22 neurons were seeded in 24-well plates and treated according to the experimental needs. Cells were stained with staining solutions prepared according to the manufacturer's protocol before or after harvest. For the measurement, medium over the cells was collected in a separate 1.5 mL Eppendorf Safe-Lock reaction tube for each well, wells were washed with 0.3 mL PBS/well, which was also collected in the corresponding tubes. Cells were carefully harvested using an unsterile trypsinization solution. After microscopically detected cell detachment, the reaction was stopped with the corresponding solutions from the tubes and the suspension was centrifugated at 2,000 rpm for 5 min. The supernatant was sucked away and a washing step with centrifugation in 0.3 mL of PBS/well was prepended before suspension in PBS or the staining solution. The volume for the final solution was chosen according to cell density (150–500 µL). For the analysis the cell density in the capillary shouldn't exceed 500/µL, as signals might get distorted. The samples were kept on ice until measurement by flow cytometry using the Guava EasyCyteTM Flow Cytometer (Merck Millipore, Darmstadt, Germany). Data were collected from 5,000 cells with three replicates per condition.

2.4.2 Apoptosis Detection

After the harvest cells were resuspended in 130 µL staining solution prepared by dilution of 20 µL Annexin V-FITC (fluorescein isothiocyanate) and 20 µL propidium iodide in 3.5 mL 1X Annexin V Binding Buffer. Defined calcium and salt concentrations (provided in the binding buffer) are required for optimal staining. Annexin V is a 35-36 kDa Ca^{2+}-dependent phospholipid-binding protein with high affinity for phosphatidylserine (PS). It is conjugated to fluorochromes like fluorescein isothiocyanate. Usually there is no PS on the outer cell membrane. Its translocation from the cytoplasm-facing side to the outer side of the plasma membrane is one of the earlier events of apoptosis. PI is a cell-impermeable DNA intercalating dye, which enters only through ruptured membranes of late apoptotic or necrotic cells. Therefore, one can distinguish three cell populations: healthy cells (AV-/PI-), early apoptotic cells (AV+/PI-) and late apoptotic and necrotic cells (AV+/PI+). DNA degradation by endonucleases, which happens in a characteristic

manner in apoptotic cells and varies in intensity depending on the lethal insult in necrotic cells, leads to a reduction of PI fluorescence over the course of time. Annexin V-FITC/PI was excited with a 488 nm laser (blue) and emission was recorded with a 525/30 nm filter (green) and a 690/50 nm filter (red).

2.4.3 Detection of lipid peroxides

Before harvest, each well was incubated with 1 µL BODIPY 581/591 undecanoic acid stock solution for 1 h at 37 °C. Then, cells were harvested as described above (see 2.4.1). Lipid oxidation is a recognized end point for the study of oxidative stress. BODIPY enters the lipid bilayer, where its polyunsaturated butadienyl segment is subject to oxidation by oxyl-radicals together with the endogenous fatty acids. When attacked by reactive oxygen metabolites it undergoes a fluorescence shift from red (590 nm) to green (510 nm) fluorescent emission. This shift can be triggered only by oxy-radicals and not by superoxides, nitric oxides, transition metal ions and hydroperoxides. BODIPY was excited at 488 nm and its emission was detected using a 525/30 nm band pass filter for green and a 690/650 nm band pass filter for red.

2.4.4 Measurement of mitochondrial ROS formation

Cells were harvested as described above (see 2.4.1). The pellet of each tube was incubated with a 1:1,000 dilution of 5 µM MitoSOX Red stock solution in PBS for 0.5 h in an insterile incubator. To avoid background noice, the staining solution was exchanged for PBS after centrifugation.
MitoSOX Red is a live-cell permeable selective indicator of mitochondrial superoxide (O_2^-) production. The cationic triphenylphosphonium substituent is responsible for the mitochondrial membrane potential driven uptake of the probe in actively respiring mitochondria. Apoptotic cells stain more weakly with this dye due to the loss of membrane potential. The dye efficiently competes with superoxide dismutase (SOD) for superoxide and exhibits a fluorescence excitation peak at around 400 nm, that is specific for the ethidium oxidation product generated only by superoxide. The fluorescence is exhibited while binding to nucleic acids. Excitation of MitoSOX red dye was at 488 nm and emission was recorded via a 690/50 nm band pass filter.

2.4.5 Evaluation of mitochondrial membrane potential ($\Delta\Psi$m)

Before harvest, each well was incubated with 1 µL MitoPT TMRE kit stock solution for 30 min at 37 °C. Then, cells were harvested as described above (see 2.4.1).
Tetramethylrhodamine ethyl ester (TMRE) is a lipophilic cationic fluorescent dye which accumulates in negatively charged mitochondria proportionally to the $\Delta\Psi$m making it a valuable tool to evaluate mitochondrial viability and function. The $\Delta\Psi$m is generated

by proton pumps (complexes I, III and IV) and is the major component of the proton motive force that determines the maximal available rate of ATP formation. The intensity of fluorescence varies due to alterations in energy metabolism (when matched with cell respirometry), e.g. by uncoupling agents or decreased activities of respiratory complexes or ATP synthesis/transport while a total dissipation of the $\Delta\Psi$m indicates mitochondrial membrane permeabilization during apoptosis. Fluorescence was excited with a 488 nm laser (blue) and emission recorded with a 690/50 nm filter (red).

2.5 Statistical analysis

All data are given as mean $\pm$ or $+$ standard deviation (SD) from at least 2 independent experiments, if not declared otherwise, in which all treatment conditions were assayed at least in triplicate.

Differences between groups were evaluated by one-way ANOVA with MS Excel. Significant main effects were further analysed by Scheffé's post-hoc test in MS Excel with the formula

$$F_{Scheff\acute{e}'s} = \frac{\frac{1}{m-1}(\overline{X}_i - \overline{X}_j)^2}{S^2(\frac{1}{n_i} + \frac{1}{n_j})} \sim F_{m-1,n-m}$$

where $\overline{X}_i$, $\overline{X}_j$ are sample means of groups with sizes n_i, n_j correspondingly, S^2 $-$ is the within-group variation and m $-$ the amount of groups. Scheffé's distribution follows Fisher's statistics with the degrees of freedom $m-1$ and $n-m$.

Differences between groups were considered statistically significant when $p < 0.05$.

Chapter 3

Results

This section will give the findings of the practical work and is divided into two parts: first, experiments performed in cotreatment mode, which means that phenformin and cell death inducers were added on the cells simultaneously and second, the ones in pretreatment mode, where cells were pre-incubated with phenformin for 24 h and the cell death inducer was added afterwards for another incubational period of up to 22 h.

3.1 Cotreatment

3.1.1 Glutamate and phenformin both lower metabolic activity in the MTT assay

The MTT assay is used as a preliminary cell viability assay. Cells with a low metabolism reduce very little MTT. The reduction depends on the cellular metabolic activity due to NAD(P)H flux. Since this reaction doesn't happen in dead cells, the assay correlates with cell viability.
In a preliminary experiment HT22 cells were treated with varying concentrations of glutamate (1–8 mM) with or without the addition of 250 μM phenformin and metabolic activity was measured after 16 h to establish the sensitivity of HT22 cells towards glutamate (Fig. 3.1). All glutamate concentrations proved cytotoxic. Glutamate toxicity was concentration dependent with 1 mM glutamate showing a drop in metabolic activity of about 50% and concentrations > 6 mM showing levels under 25% compared to control levels. Metabolic activity was also significantly reduced by phenformin alone by 50% of control levels. Phenformin couldn't rescue the cells from death by glutamate in any of the tested concentrations.
Furthermore, a concentration series of phenformin from 0.1 μM to 1 mM was generated with a 16 h treatment time (data not shown). The effect of phenformin on metabolic activity was concentration-dependent and started at 100 μM. No used concentration lowered metabolic activity under 60% of control level. While phenformin concentrations, that had

no effect on metabolic activity, didn't show any protection from glutamate, concentrations > 100 µM showed a slight, concentration-dependent rescue of metabolic activity from glutamate. But since the metabolic activity under protection was still lower than 30%, this cannot be interpreted as a significant effect in the case of the MTT assay.
The emerged question, if there are transiently more significant protective effects, had to be elucidated. For this, the MTT assay was performed at 5 different time points, namely at 8, 10, 12, 14 and 16 h after treatment (Fig. 3.2). When comparing different time points in the MTT assay one can see that the glutamate-treated cells die progressively. But the most pronounced drop of cell viability finds place between 10 and 12 h of exposure time. 12 and 14 h after treatment, the phenformin-treated groups indeed had an almost 50% higher survival rate compared to glutamate-only-treated groups (51 vs. 27%).

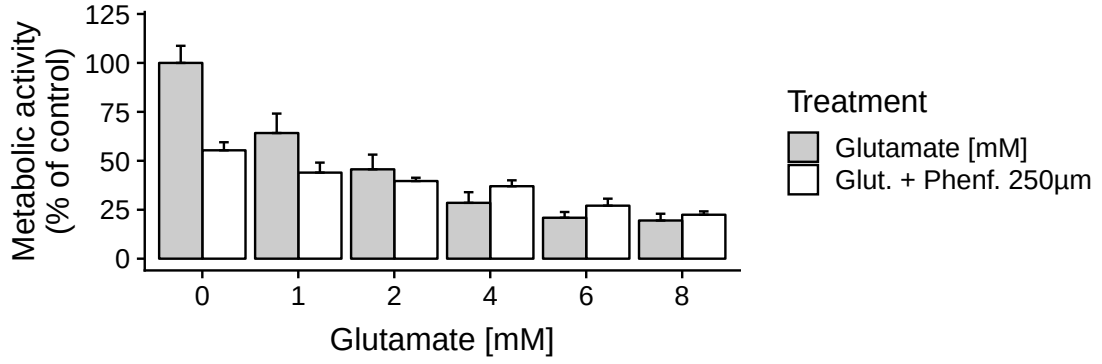

Figure 3.1: Concentration-dependent decrease of metabolic activity by both glutamate and phenformin. The MTT assay after 16 h exposure of 1–8mM glutamate and 250 µM phenformin showed that both glutamate and phenformin lead to a concentration-dependent decrease of metabolic activity. Phenformin showed no protection against glutamate. (n=8/treatment condition, experiment performed one time). Glut.: Glutamate, Phenf.: Phenformin

Following AV/PI-FACS measurements confirmed the transient nature of protection and excluded cytotoxic effects for phenformin concentrations up to 1 mM 16 h after treatment (see 3.1.3). The effect seems to reach a plateau at 60% metabolic activity of control level after 14 h.
All glutamate concentrations exerted cytotoxic effects. Glutamate toxicity was concentration dependent with 1 mM glutamate showing a drop in metabolic activity of about 50% and concentrations > 6 mM showing survival rates below 25% compared to controls . Metabolic activity was also significantly reduced by phenformin alone to 50% of control levels. Phenformin could not rescue the cells from death by any of the tested glutamate concentrations. Furthermore, a concentration range of phenformin starting at 0.1 µM and going up to 1 mM was tested in the MTT assay after a 16 h treatment (data not shown). The effect of phenformin on metabolic activity was concentration-dependent and started at 100 µM. None of the applied concentrations lowered metabolic activity below 60% of control level. While phenformin concentrations that had no effect on metabolic activity did not show any protection from glutamate, concentrations > 100 µM showed a slight, concentration-dependent increase of metabolic activity. Since the metabolic activity was

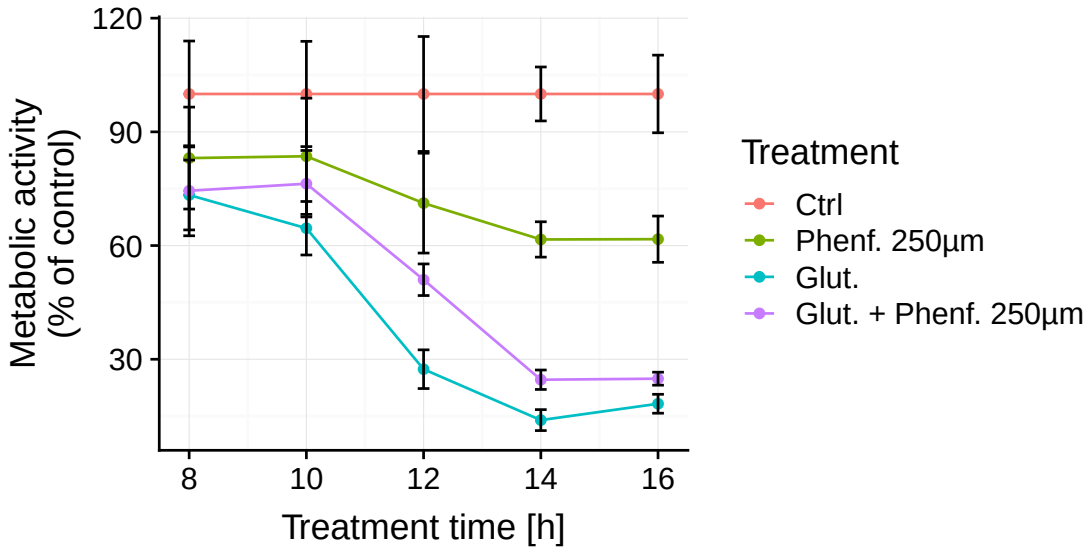

Figure 3.2: Progressive decline of metabolic activity under glutamate treatment and transient protection by phenformin. The MTT assay with 8, 10, 12, 14 and 16 h timepoints showed progressive decline of metabolic activity under glutamate treatment (8 mM) 250 µM phenformin decreased metabolic activity to reach a plateau at 60% after 14 h. At a 12 h timepoint a transient protection appeared. (n = 8/treatment condition, 2 independent experiments). Data are given as mean $\pm SD$). Ctrl: control, Phenf.: phenformin, Glut.: glutamate

still lower than 30% in protected cells, this cannot be interpreted as a significant effect using the MTT assay.

The emerging question, if there are transiently more significant protective effects, had to be elucidated. For this, the MTT assay was performed at 5 different time points, namely at 8, 10, 12, 14 and 16 h after treatment When comparing different time points in the MTT assay it was observed that the glutamate-treated cells died progressively in a time dependent manner. But the most pronounced drop of cell viability takes place between 10 and 12 h of exposure time. According to this assay, 12 h and 14 h after treatment, the phenformin-treated groups indeed had an almost 50% higher survival rate compared to glutamate-only-treated groups (51 vs. 27%). The following AV/PI-FACS measurements confirmed the transient nature of protection and excluded cytotoxic effects for phenformin concentrations up to 1 mM determined at 16 h after onset of treatment. The metabolic effect seemed to reach a plateau at 60% metabolic activity of control level after 14 h.

3.1.2 Phenformin reduces growth rates and shows transient protection against glutamate toxicity

Antiproliferative effects were microscopically observable. Quantitative analysis of cytotoxic and antiproliferative effects was conducted with xCELLigence RTCA. Since it has already been established in the MTT assay that phenformin slows down cell metabolism, antiproliferative effects were expected.

Addition of glutamate (8 mM) is indicated by time point “0 h” in the graph (Fig. 3.3).

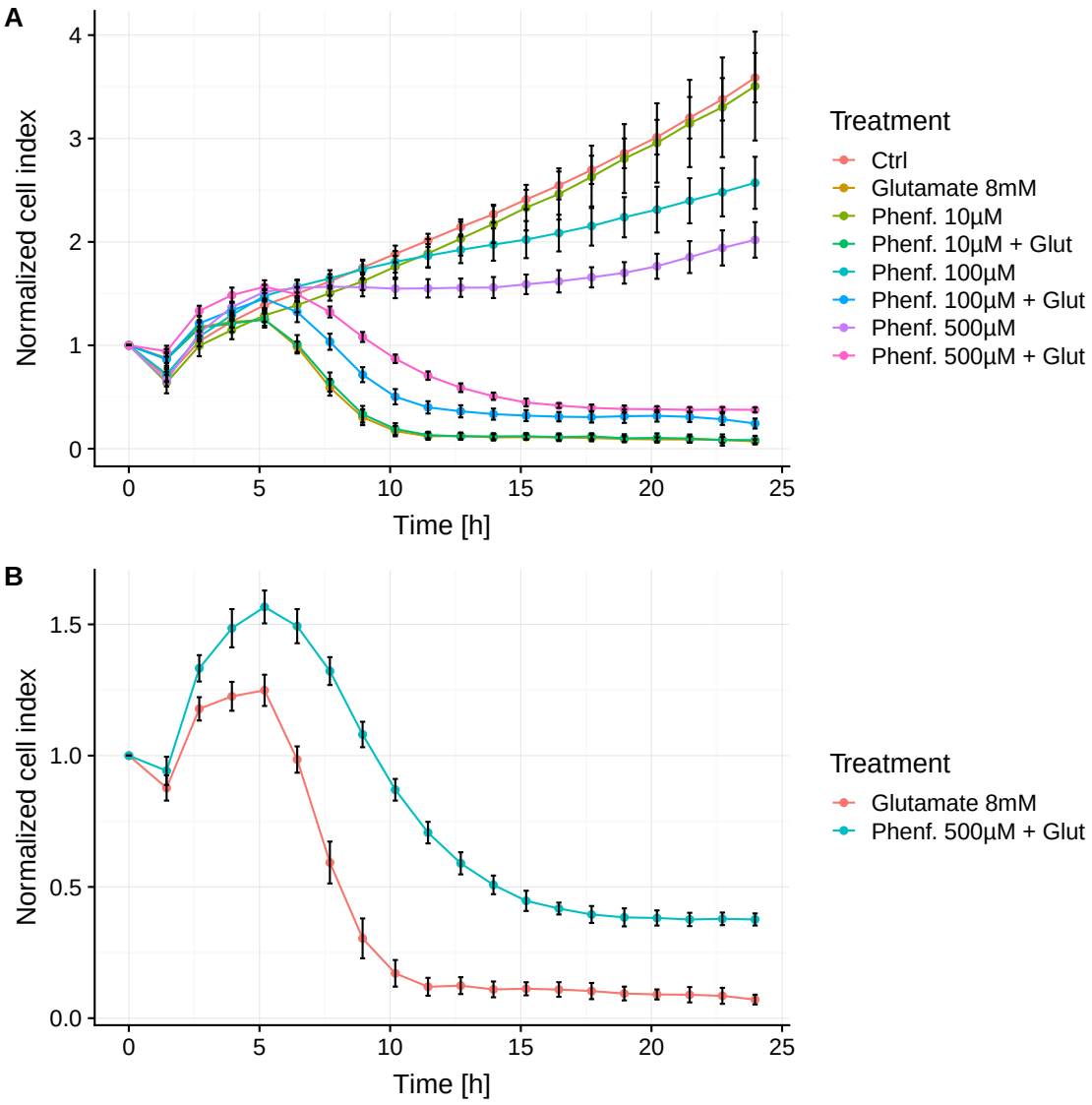

Figure 3.3: Cytotoxicity of glutamate, reduced growth rates and transiently protective effects of phenformin. A: Real-time impedance measurements showed reduced proliferation with phenformin concentrations > 100 µM. Glutamate induced cell death between 5 and 10 h exposure time. The transient protection of phenformin was concentration-dependent. **B:** The treatment group with highest protection (500 µM phenformin) was selected to form a separate graph for better visualisation. (n = 6/treatment condition, 3 independent experiments). Data are given as mean ±*SD*. Ctrl: control, Phenf.: Phenformin, Glut: glutamate

Cell death became detectable 5–6 h after the onset of the glutamate challenge. After initiation of cell death the HT22 cells died within 4–5 h. In contrast, the control group showed an increase of NCI, caused by its steady proliferation. Phenformin concentrations of > 100 µM showed both significant antiproliferative effects and significant transient protection against 8 mM glutamate. The effect was concentration dependent, with phenformin concentrations > 750 µM showing decreasing protection (data not shown). As in the MTT assay, the phenformin concentrations that did not have inhibiting effects on proliferation were also not protective against glutamate. The NCI's of the phenformin treated groups (> 100 µM) didn't have such a sharp decline as the glutamate exposed group. Al-

though it seems that the phenformin-treated groups stabilize around a higher value than the glutamate-only group, this NCI is nevertheless far below the control NCI, also the AV/PI experiments clearly show a loss of protection after 16 h cotreatment.

3.1.3 Phenformin delays neuronal cell death induced by both glutamate and erastin

In order to rule out cytotoxic effects of phenformin and to show cell survival without distortion by reduced growth rates cells were stained with Annexin V-FITC to quantify early apoptotic cells and with PI to quantify late apoptotic and necrotic cells. Cells were exposed to glutamate or erastin for 10, 12 and 16 h. The experiments were run with erastin in order to investigate the transient protection with another cell death inducer. The BID-inhibitor BI-6c9 was used as a positive control for protection against cell death. Annexin V/PI staining and subsequent FACS analysis showed the time-dependent progression of cell death induced by glutamate, while erastin had achieved its maximal damaging effect already after 10 h (Fig. 3.4 and Fig. 3.5). Protection by phenformin and metformin against glutamate- and erastin-induced cell death was proven to be transient with cell death being merely delayed by about 6 h in the case of erastin, while in the case of glutamate the delay lasted longer, however, at the 16 hour timepoint protection was lost in most of the experiment replications. The BID-inhibitor BI-6c9 inhibited cell death with highest potency at all timepoints. Phenformin and metformin showed comparable effects at a concentration of 250 µM and 20 mM, respectively, making phenformin the more potent of the two. The cytotoxic effects of the phenformin- and metformin-control groups should be considered as unfortunate artefacts or they might have to do with the stability of the drugs in the added solutions (solution with many freeze-thawing cycles).

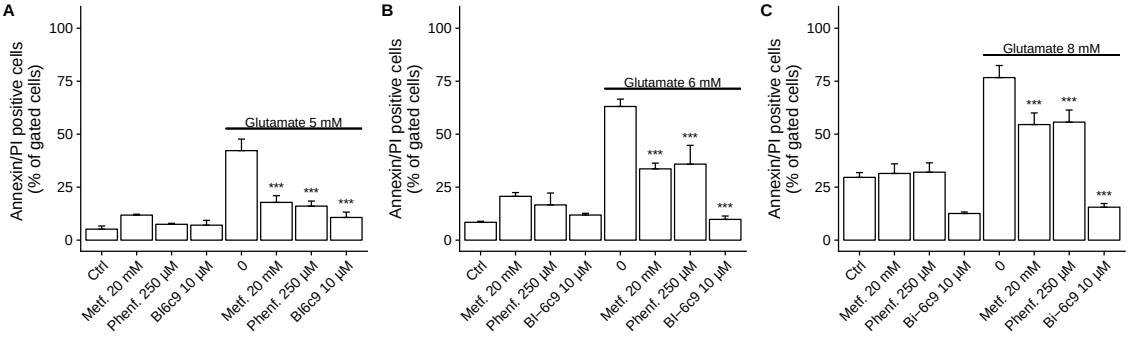

Figure 3.4: Delay of glutamate-induced cell death by phenformin. AnnexinV/PI staining and subsequent FACS analysis 10, 12 and 16 h after treatment showed a delay of glutamate-induced death (5–8mM) by phenformin (250 µM) and metformin (20mM). The amount of AV/PI positive cells is increasing linear and the delay of cell death is taking longer with glutamate compared to erastin. The BID-inhibitor BI-6c9 inhibited cell death at all time-point. (n = 3/treatment condition, experiment performed once) All data are given as mean $+SD$, $^{***}p < 0.001$ compared to glutamate-treated HT22 control (ANOVA, Scheffé´s test). Ctrl: control, Metf.: metformin, Phenf.: phenformin

.

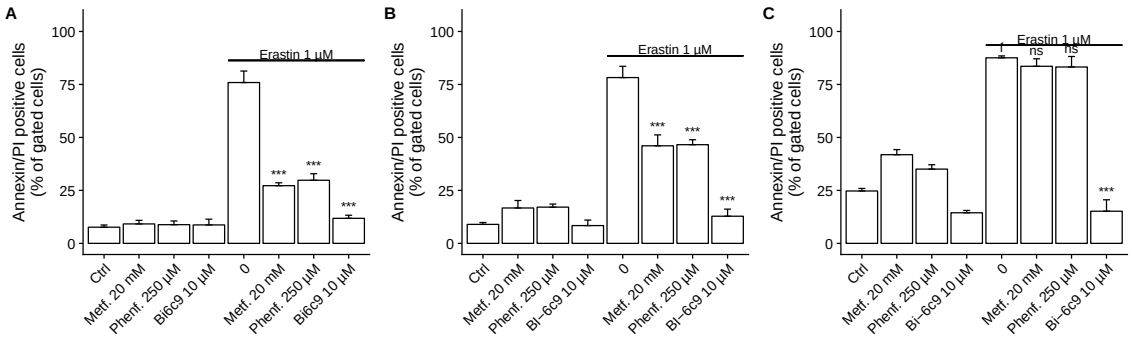

Figure 3.5: Delay of erastin-induced cell death by phenformin. AnnexinV/PI staining and subsequent FACS analysis 10, 12 and 16 h after treatment showed a delay of erastin-induced death (1 µM) by phenformin (250 µM) and metformin (20 mM). The protection was completely abolished after 16 h. The BID-inhibitor BI-6c9 inhibited cell death at all time-point. (n = 3/treatment condition, experiment performed once). All data are given as mean $+SD$, $^{***}p < 0.001$ compared to erastin-treated HT22 control (ANOVA, Scheffé´s test.). Ctrl: control, Metf.: metformin, Phenf.: phenformin

.

3.1.4 Phenformin slows glutamate-induced accumulation of lipid peroxides

Glutamate induces the formation of lipid peroxides. Accumulation of lipid peroxides leads to malfunction and death of the cell. Lipid peroxidation measurements were performed 7–9 h after treatment. Lipid peroxidation was also observed with erastin (data not shown). Phenformin lead to a modest attenuation of lipid peroxidation in the dying cells (Fig 3.6).

3.1.5 Phenformin lowers glutamate-induced mitochondrial superoxide production

The MitoSOX staining was performed once after 8 h of treatment, but there was only a slight glutamate-induced increase of ROS detectable. After 16 h of glutamate exposure the damage was sufficient to show the concentration-dependent decrease of mitochondrial ROS by phenformin concentrations >50 µM (Fig. 3.7). Notably, there seemed to be a slight concentration-dependent increase of ROS by phenformin itself. The phenformin concentrations with the apparently higher mitochondrial superoxide levels were also the ones with better protection against glutamate-induced mitochondrial ROS increase.

3.1.6 Phenformin lowers the mitochondrial membrane potential

TMRE accumulates in healthy mitochondria in an MMP dependent manner and its fluorescence decreases proportionally with a decrease of the MMP due to redistribution into the cytosol. A total dissipation of the MMP is an indicator of apoptosis. Phenformin has

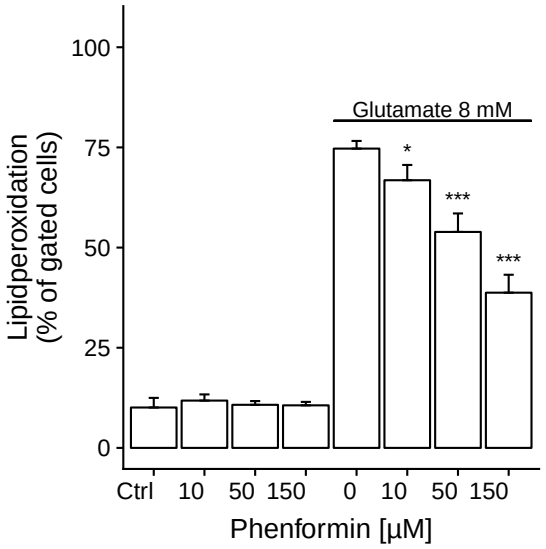

Figure 3.6: Phenformin decreased levels of lipid peroxidation. Bodipy staining and subsequent FACS analysis after 9 h of treatment revealed that phenformin decreased glutamate-mediated (8mM) lipid peroxidation in a concentration-dependent manner (10–150 µM). (n = 3/treatment condition, 3 independent experiments). Data is given as mean $+SD$, $^{***}p < 0.001$, $^{*}p < 0.05$ compared to glutamate-treated HT22 control (ANOVA, Scheffé´s test).

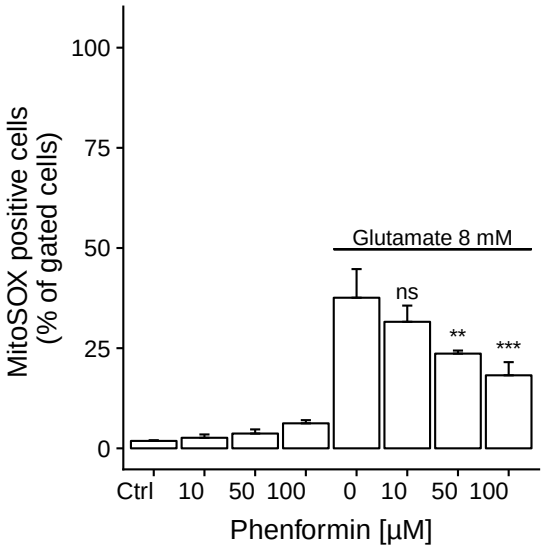

Figure 3.7: Attenuation of mitochondrial ROS by phenformin. MitoSOX staining and subsequent FACS analysis after 16 h of treatment revealed that phenformin attenuates mitochondrial ROS generation after glutamate exposure (8mM) in a concentration-dependent manner. (n = 3/treatment condition, 2 independent experiments). Data is given as mean $+SD$, $^{***}p < 0.001$, $^{**}p < 0.01$ compared to glutamate-treated HT22 control (ANOVA, Scheffé´s test).

proven to be a MMP lowering substance. The effect was detected at all measured time points (8 and 16 h) and was time- and concentration-dependent, with the maximal effect detected as a 20% drop by > 100 µM after 16 h (Fig. 3.8). After 8 h exposure time to glutamate, the MMP is decreased by only 10% compared to control level, while after 16 h it dropped by 50%. Remarkably, the MMP lowering effects of glutamate and phenformin added up and the combination of the two had lower TMRE fluorescence levels than gluta-

mate alone. Interestingly, the concentrations of phenformin with stronger MMP decrease were also more effective in delaying cell death (see 3.1.3).

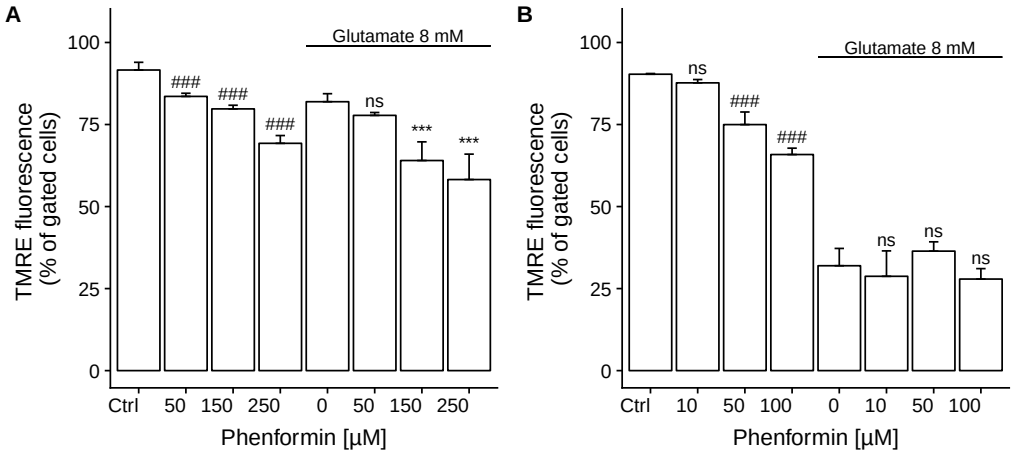

Figure 3.8: MMP lowering effect of phenformin. TMRE staining and subsequent FACS analysis revealed a concentration-dependent MMP lowering effect of phenformin and no protection against glutamate induced MMP dissipation. **A:** after 8 h treatment (n = 3/treatment condition, experiment performed once) **B:** after 16 h treatment. (n = 3/treatment condition, 2 independent experiments) All data are given as mean $+SD$, $^{\#\#\#}p < 0.001$ compared to untreated HT22 control; $^{***}p < 0.001$, ns (non significant) compared to glutamate-treated HT22 control (ANOVA, Scheffé´s test).

3.2 Pretreatment

3.2.1 Phenformin increases the survival of glutamate-damaged cells

Within the 24 h pretreatment time, phenformin concentrations < 25 µM showed slightly decreased proliferation rate compared to control, while concentrations > 100 µM led to reduced proliferation below detection levels (Fig. 3.9). After adding the glutamate solution and thus diluting the phenformin concentrations in all wells by 50% the proliferation rate became a bit steeper in all phenformin-treated groups. Glutamate-induced cell death was again detectable after 7–8 h and had a steep decline, while phenformin-treated groups (> 10 µM) did not undergo the massive cell death and instead showed a mild reduction of NCI, which stayed over glutamate-only levels till the end of the experiment (longest measured time: 68 h), however the high standard deviation after such long treatment time deprives the results of their significance.

The AV/PI FACS analysis ruled out cytotoxic effects of phenformin (10–100 µM) after 44 h of incubation (Fig. 3.10). Phenformin concentrations as low as 10 µM showed significant protection against glutamate-induced cell death.

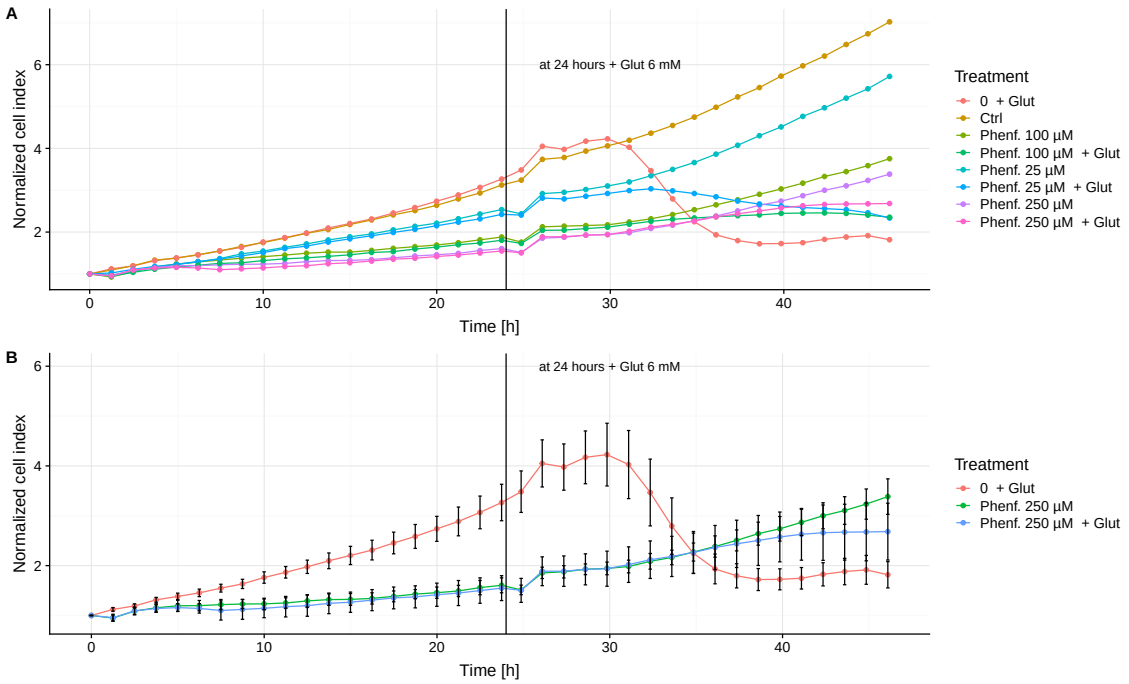

Figure 3.9: Antiproliferative and permanent protective effects of phenformin. A: Real-time impedence measurements showed a concentration-dependent reduction of proliferation by phenformin. Phenformin-treated cells didn't undergo the massive cell death between 8–10 h after glutamate exposure (6 mM). For better visualisation the standard deviations were not added. **B:** The treatment group with highest protection (250 µM phenformin) was selected from the same experiment to form a separate graph for better visualisation. (n = 6/treatment condition, 2 independent experiments). Data are given as mean $\pm SD$). Ctrl: control, Phenf.: phenformin, Glut: glutamate

3.2.2 Phenformin lowers glutamate-induced lipid peroxide formation

The high lipid peroxide level of the glutamate group indicates a timepoint after or during the exponential phase of ROS accumulation which is effectively suppressed by phenformin (Fig. 3.11).

3.2.3 Phenformin lowers glutamate-induced mitochondrial superoxide levels

The measurements of mitochondrial superoxide levels after 24 h pretreatment and 17 h of exposure to glutamate showed that phenformin lowered ROS levels significantly (Fig. 3.12). The glutamate-induced production of mitochondrial ROS was attenuated in a concentration-dependent manner at concentrations > 10 µM phenformin. As in the cotreatment experiments, phenformin showed a slight but not further evaluated increase of mitochondrial ROS.

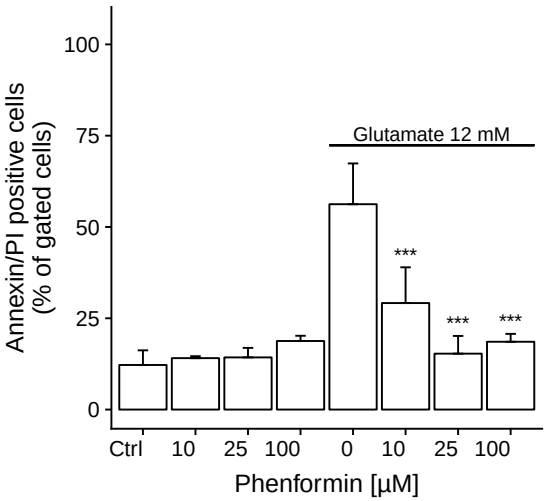

Figure 3.10: Phenformin inhibits cell death. AV/PI staining and subsequent FACS analysis showed a decrease of glutamate-induced cell death (12 mM, 20 h) to control levels after a 24 h pretreatment with 25–100 µM phenformin. (n = 3/treatment condition, 3 independent experiments) Data are given as mean $+SD$, $^{***}p < 0.001$ compared to glutamate-treated HT22 control (ANOVA, Scheffé´s test)

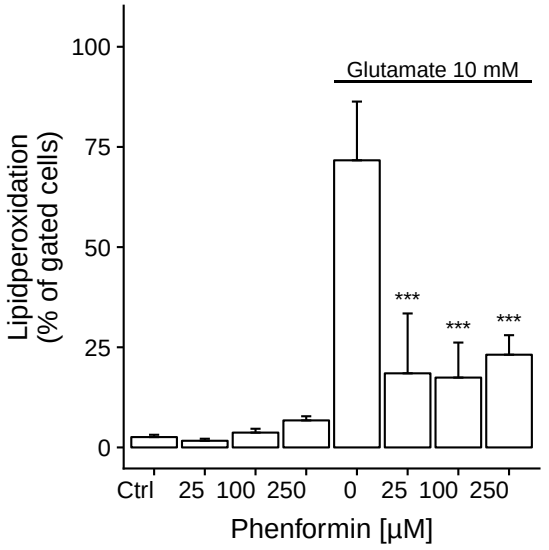

Figure 3.11: Strong reduction of lipid peroxidation by phenformin. Bodipy staining and subsequent FACS analysis showed a drop of glutamate-induced lipid peroxidation (10 mM, 18 h) by 25–250 µM phenformin (24 h pretreatment). (n = 3/treatment condition, 3 independent experiments) Data is given as mean $+SD$, $^{***}p < 0.001$ compared to glutamate-treated HT22 control (ANOVA, Scheffé´s test)

The phenformin concentrations with higher MitoSOX fluorescence levels were also more protective against glutamate-induced mitochondrial ROS production (34 h incubation, data not shown).

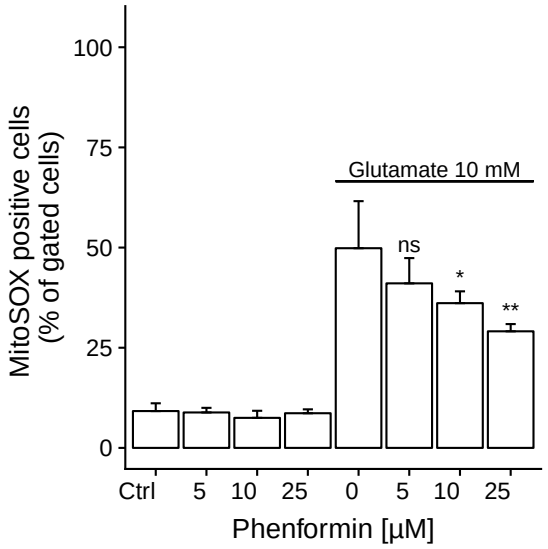

Figure 3.12: Phenformin decreases mitochondrial superoxides. MitoSOX staining and subsequent FACS analysis showed a concentration-dependent decrease of mitochondrial ROS generation by phenformin (24 h pretreatment) in glutamate-damaged cells (10 mM, 17 h). (n = 3/treatment condition, 3 independent experiments). Data is given as mean $+SD$, $^{**}p < 0.01$, $^{*}p < 0.05$, ns (non significant) compared to glutamate-treated HT22 control (ANOVA, Scheffé´s test.)

3.2.4 Phenformin lowers the $\Delta\Psi$m and shows protection against glutamate at 25 µM

17 h of exposure to glutamate decreased the MMP only moderately (Fig. 3.13). 25 µM phenformin brought the MMP of glutamate-damaged cells back to levels of the corresponding phenformin-only treated group. There seemed to be a concentration-dependent decrease of the MMP by phenformin here as well, although that not always detectable.

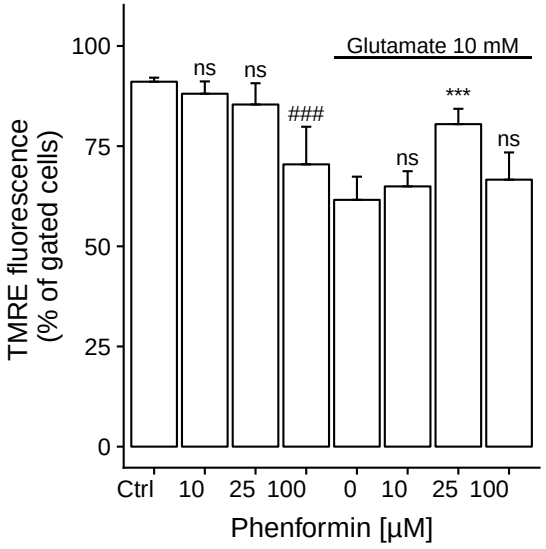

Figure 3.13: Effects of phenformin on the MMP. TMRE staining and subsequent FACS analysis showed an MMP lowering effect of phenformin (100 µM, 41 h treatment) and a significant increase of the MMP in glutamate-damaged cells (10mM, 17 h) by 25 µM phenformin in pretreatment mode. (n = 3/treatment condition, 2 independent experiments). Data is given as mean $+SD$, $^{\#\#\#}p < 0.001$ compared to untreated HT22 control; $^{***}p < 0.001$, ns (non significant) compared to glutamate-treated HT22 control (ANOVA, Scheffé´s test)

Chapter 4

Discussion

Experimental design

The HT22 cell model system is a well-established system to identify neuroprotective agents. The oxidative stress induced in this model is not due to externally applied oxidants, as for example H_2O_2 or iron(III) sulfate, but rather mediated by ROS generated by endogenous metabolic processes within the cell [134] and thus this model might be more closely related to oxidative stress occurring in vivo. Tan et al. (2001) reported that glutamate-induced ROS-formation starts approx. 5–6 h after exposition to glutamate and that maximal ROS values are reached after 10 h [20]. This was the basis for choosing time points for the experiments in the present study. However, in practice, choosing the best timepoints proved not that easy, as effects varied between different experiments. Influencing factors might have been passage number, confluency or spontaneous resistence. The effects of biguanides strongly depend on the metabolic substrate availability of the cells and this could be another influencing factor [135]. For the total inhibition of cystine uptake, concentrations of extracellular glutamate as low as 100 μM were described, which is well below the level of extracellular glutamate found in models of stroke and trauma [21]. It should be noted, that in the experiments much higher glutamate concentrations were used (8–12 mM). The decreased sensitivity might also be explained by the above mentioned influencing factors like spontaneous resistance. The long incubation times and almost empty wells with hardly proliferating cells after the phenformin treatment, compared to the overgrown control wells created very unequal culture conditions. Maybe an adjusted cell seeding number would have been a better variant. Of note, glutamate resistance depending largely on the confluency of the cells has been described earlier [136], and may be a major reason for the very high glutamate concentrations used in the present experiments.

Studies on phenformin in neuronal cell systems are scarce and there is no published data on phenformin in the oxytosis model in HT22 cells to date. Despite the prominent effects of phenformin on cell proliferation and basal metabolic activity, we decided to use this

biguanide for the experiments because in cellular systems it reproduces most of the desired metabolic effects of metformin but more potently. The higher potency of phenformin resulted in a protective concentration in the micromolar range, while metformin concentrations with comparable protective effects were in the millimolar range. The phenformin concentrations used in the experiments vary with a factor of 1,000. This is due to the fact that protective effects in cotreatment mode up to 24 h were visible in the range of > 100 μM up to 750 μM (in the xCELLigence experiments), whereas in the pretreatment mode, phenformin concentrations between 5 and 25 μM were already protective, although also here concentrations of 100–250 μM sometimes showed stronger protective effects. I would suggest phenformin concentrations of around 5–50 μM for HT22 cells with incubation times > 40 h, which already show sufficient protection from glutamate toxicity. The question, why shorter incubation time periods in the cotreatment experiments required higher phenformin concentrations (optimum > 250 μM) as compared to the pretreatment (optimum 25 μM), remains unsolved and might be due to the pharmacokinetics of the substance or due to the activation of some additional cellular processes.

The initial decision to include a pretreatment with phenformin resulted from the moderate and only transient protective effects on mitochondrial parameters and cell viability and the hypothesis that effects might be of a more durable nature after a pretreatment time. This assumption was clearly supported by the obtained results from the pretreatment experiments, where phenformin showed more pronounced protective effects compared to cotreatment protocols. In particular, after the pretreatment phenformin had stronger protective effects on cell viability and mitochondrial parameters and these were lasting longer than when used in cotreatment mode, indicating different mechanisms of protection. However, the time window of protection after pretreatment is currently unknown and may not be permanent neither.

Antiproliferative effects and metabolic reprogramming

The antiproliferative effect mediated by phenformin was partly interfering with the interpretation of the results. Cell viability as the key outcome parameter of interest was detected by the MTT assay and the xCELLigence-based impedance measurements, but the antiproliferative effect impeded the discovery of significant protective effects. On the other hand, the interdependency of decreased metabolism and cytoprotective effects was demonstrated, as only metabolically suppressed cells showed protection against glutamate. There is valid proof that enhancing glycolysis leads to neuroprotection [137–139] and glycolysis might be the explanation for the protective effect of phenformin in this cell model system.

Effect on mitochondrial superoxide and lipid peroxide formation

Although GSH levels were not measured in the present study, the initial GSH loss and concomitant ROS elevation due to GPX4 deactivation is probably not remarkably affected by phenformin, as lipid peroxidation levels increase to a certain level over control level in all treatment scenarios, with the lowest achieved effect being 20% over control levels in the pretreatment experiments. However, mitochondrial GSH levels might be elevated due to the inhibition of mitochondrial metabolism. It is thus concluded that phenformin delays or ameliorates lipid peroxidation at a later stage of the oxytosis cascade. It has been frequently described that the accumulation of lipid peroxides happens in two phases with a mitochondrial involvement in the second, exponential burst of ROS formation. Since the late lipid peroxidation burst was suppressed by pretreatment with phenformin, a mechanism of action at the level of mitochondria is proposed.

The MitoSOX results indicate that phenformin lowered superoxide formation during oxidative stress. Phenformin also mildly increased mitochondrial superoxide levels, and this effect increased the resistance towards glutamate. CI is a major producer of ROS within a cell. Its role in oxidative stress is firmly validated [140]. In the context of oxidative stress, the shift from respiration to glycolysis has been proven cytoprotective as the oxidative burden for the cell decreases. However, mROS play a dual role as they are vital signalling molecules for the induction of a stress-response [141,142]. Another level of complexity is added by the need to differentiate between the various sites of ROS formation as each site even at one complex supposedly encodes for a different signal and has different consequences [143]. The exact mechanism of mROS generation during oxytosis is not known, but Ca^{2+} plays a major role [144]. A mitohormetic ROS signal for the upregulation of the antioxidant defense has not conclusivelly been proven for metformin and phenformin. If the slight elevation of mitochondrial superoxide levels by phenformin in my experiments can be interpreted as such a mitohormetic signal needs further evaluation. Nevertheless, in the context of oxidative stress the shift from respiration to glycolysis represents an undermined cytoprotective strategy under many laboratory conditions [145]. However, due to the more pronounced effect on lipid peroxidation as compared to the effect on mitochondrial superoxide formation in the pretreatment mode, it might be that the responsible mechanism after all has an extra-mitochondrial explanation, like increased cellular radical scavenging capacity [146] or altered iron content [147, 148]. Especially an altered lipid composition might have decreased the oxidizable pool and resulted in lower lipid peroxide levels [65].

Effect on mitochondrial membrane potential

$\Delta\Psi m$ is generated by proton pumps (complexes I, III and IV), which generate the proton motive force that determines the maximal available rate of ATP formation. An $\Delta\Psi m$

lowering effect of a complex I inhibiting agent might thus seem a logical consequence. This is not always the case, as the mitochondrion is capable of maintaining a physiological or even slightly elevated $\Delta\Psi m$ in response to $\Delta\Psi m$ threatening insults. This is achieved by reversal of the ATP synthase, which pumps protons out upon ATP expenditure. HT22R, for example, were found to endure ineffective energy metabolism in the form of reverse activity of the ATP synthase to protect their membrane potential during oxidative stress [57]. As early as 8 h after glutamate treatment, there is a small detectable decrease of the $\Delta\Psi m$. After 16 h the dissipation of TMRE fluorescence might already indicate total destabilization of the mitochondria. Phenformin had a concentration-dependent $\Delta\Psi m$ lowering effect of max. 20% below control level. Remarkably, in cotreatment mode the $\Delta\Psi m$ lowering effects of phenformin and glutamate added up. One would suppose that as a result the cells under both phenformin and glutamate exposure were more prone to cell death. This didn't seem to be the case, when looking at the AV/PI results. In the pretreatment mode, the $\Delta\Psi m$ also seemed to be slightly lowered by phenformin, but unfortunately only in one replication, thus more experiments would be needed here. In one series of experiments, the 100 µM concentration of phenformin acted cytotoxic also in the AV/PI and MitoSOX measurements, thus the effects of phenformin pretreatment on $\Delta\Psi m$ at this timepoint should be repeated. Since the lower phenformin concentrations were protective against cell death, lipid peroxidation and mitochondrial ROS formation, it might seem that a decreased $\Delta\Psi m$ is after all not a requirement for the long-term protection after long incubation time with phenformin. Instead, effectors downstream of the mitochondria could have increased cell viability. Remarkably, there was a significant increase in the $\Delta\Psi m$ in the glutamate-exposed groups by 25 µM phenformin back to the level of the corresponding phenformin-only treated group. The high $\Delta\Psi m$ after 17 h of glutamate exposure is questionable, when comparing with all other measured parameters indicating massive damage of the cells. Also, the narrow protective concentration range of phenformin was unexpected.

A paper by Öxler et al. (2012) showed that a 9 h pretreatment with low dose rotenone, a highly potent complex I inhibitor, transiently preserved cells from glutamate toxicity. The protective effect has been associated with AIF downregulation, since complex I and AIF are supposedly influencing each others transcription. Also the protection has been associated with the observed slight mitochondrial membrane depolarization by rotenone [52]. Other researchers have also demonstrated that even a small mitochondrial depolarization is sufficient to prevent mitochondrial Ca^{2+} uptake [149–151], cytosolic Ca^{2+} signals and the downstream signalling pathway to cell proliferation [152]. An endogenous strategy of mitochondria to cope with increased amounts of ROS is uncoupling the proton gradient from energy production by proton-leaking uncoupling proteins (UCPs) [153]. Uncoupling leads to a lower membrane potential, which lowers superoxide production by RET from CI [154]. Same could be true for the mechanism of action of metformin, since an

uncoupling effect has already been discribed in the literature [155].

Effect on cell viability

The measurements of mitochondrial parameters are indirect indicators of cell viability as their aggravation prepends cell death. The AV/PI assay for apoptotic and necrotic cell labelling was chosen as an additional method to screen for cell viability. Phosphatidylserine exposure of dying cells is apparently a universal "eat me" signal also in the non-apoptotic pathway named oxytosis. When an apoptotic cell doesn't become phagocytosed, it becomes necrotic and PI enters the rupturing cell membrane [156]. Cells were AV/PI-positive, but we cannot say for sure if phenformin treated cells died via the same death pathway as untreated cells. The BID inhibitor BI-6c9 showed the strongest protection and cell death was totally inhibited both in the glutamate-, as well as erastin-treated groups and at all chosen timepoints (10–16 h). This cogently mirrors the efficacy of targeting mitochondrial pathways, even though BID translocation happens very late in oxytosis, i.e. downstream of GSH depletion and enhanced 12/15-LOX-mediated lipid peroxidation. Phenformin also proved effective in delaying cell death by glutamate and erastin in cotreatment mode, but only transiently. The stronger the damage, as was the case with erastin, the shorter the protective window. Erastin, the prototypical ferroptosis-inducing agent [157], conveys its damaging effects also through system xc^- inhibition, but additionally via free tubulin inhibition and increase of VDAC2 conductance [158]. It might also be, that phenformin would show stronger and longer-lasting effects with smaller glutamate concentrations.

In the xCELLigence experiments both in co- and pre-treatment mode phenformin-treated groups with visible protection permanently rised the NCI above glutamate-only levels, though clearly below their corresponding phenformin-only group levels. In the cotreatment mode, this finding should definitely be questioned since the AV/PI experiments clearly showed a loss of protection after >16 h cotreatment, while in the pretreatment experiments it is not clear how long-lasting the protection has been and permanent protection cannot be excluded for sure.

Chapter 5

Conclusions

Mitochondrial and metabolic pathways appear to tightly regulate the susceptibility of neurons to oxytosis. Therapeutic manipulation of energy metabolism is therefore potentially neuroprotective. The obtained data collectively indicate that phenformin promotes cell survival under detrimental oxidative stress conditions due to its metabolic effects. Apparently, during massive oxidative stress it is of advantage for the cell to rely on the less effective cytosolic glycolytic machinery as the trade-off for curbed mitochondrial ROS generation due to respiratory chain inhibition. Although the duration of protection after a pretreatment was not ascertained, the pretreatment rendered HT22 cells more resilient towards oxidative stress indicating expanded mechanisms of protection because of more adaptations within the cell. Whether these observations can help in the development of novel therapeutic approaches for the prevention of neurodegenerative diseases with biguanides remains to be investigated.

Chapter 6

Outlook

The apparent question left unanswered is if complex I inhibition was the main reason for the protection, e.g. via special ROS signalling or the decreased ROS formation by inactive CI, or if downstream events played a more important role. First, although it is a well-established fact that biguanides increase glycolysis to compensate for the energetic deficit, this thesis lacks the experimental assessment of phenformin-induced changes of metabolic fluxes. This can be done with a Seahorse XF analyser which measures glycolysis and oxidative phosphorylation simultaneously in the same cells. An accompanying measurement of ATP levels would give us a picture of the energy status of the cells. Unfortunatelly, so far not much attention was given to metformin's impact on lipid metabolism. Especially in the context of oxytosis and due to the obtained results on lipid peroxidation in the pretreatment mode, a closer look might bring novel insights and conclusions on the underlying mechanism of action. Investigations in neuronal systems have shown, that metformin, similar to other CI inhibitors, is an inhibitor of mPTP opening. Although a connection between oxytosis and mPTP opening is controversially discussed, phenformin's action on mPTP opening should nevertheless be taken into consideration. In order to prove the efficacy of phenformin in suppressing mPTP opening in cell death paradigms where the pore definitely plays a part in, like parthanatos, it would be sufficient to use H_2O_2 as toxic agent on HT22 cells. Mitochondria rapidly react to stimuli like oxidative stress or bioenergetic changes with structural remodelling as the regulation of mitochondrial dynamics occurs mostly at the posttranslational level. Oxytosis has been linked to disturbed mitochondrial fission events. Metformin, on the other hand, despite the well-characterized effects on the respiratory chain, has not sufficiently been investigated in regard to its effects on mitochondrial ultrastructure. It would be of great value to obtain data on the effects of phenformin on mitochondrial morphology and mitochondrial dynamics. In that context, mitophagy (the digestion of dysfunctional mitochondria) could be affected by phenformin.

Since Ca^{2+} plays such a central role in oxytosis, eventual effects of phenformin on intracellular and mitochondrial Ca^{2+} levels need to be elucidated. The other reason is that even slight changes of the $\Delta\Psi m$ have an effect on mitochondrial Ca^{2+} buffering capacity. Effects of phenformin on Ca^{2+} have already been studied in the past, but without clear results and on different cell lines, so one might consider to investigate these aspects in future studies.

Bibliography

[1] L. Galluzzi, I. Vitale, S. A. Aaronson, J. M. Abrams, D. Adam, P. Agostinis, E. S. Alnemri, L. Altucci, I. Amelio, D. W. Andrews *et al.*, "Molecular mechanisms of cell death: recommendations of the nomenclature committee on cell death 2018," *Cell Death & Differentiation*, vol. 25, no. 3, pp. 486–541, 2018.

[2] M. Fricker, A. M. Tolkovsky, V. Borutaite, M. Coleman, and G. C. Brown, "Neuronal cell death," *Physiological reviews*, vol. 98, no. 2, pp. 813–880, 2018.

[3] T. Müller, C. Dewitz, J. Schmitz, A. S. Schröder, J. H. Bräsen, B. R. Stockwell, J. M. Murphy, U. Kunzendorf, and S. Krautwald, "Necroptosis and ferroptosis are alternative cell death pathways that operate in acute kidney failure," *Cellular and molecular life sciences*, vol. 74, no. 19, pp. 3631–3645, 2017.

[4] L. Galluzzi, O. Kepp, and G. Kroemer, "Mitochondrial regulation of cell death: a phylogenetically conserved control," *Microbial Cell*, vol. 3, no. 3, p. 101, 2016.

[5] V. Rangaraju, T. L. Lewis, Y. Hirabayashi, M. Bergami, E. Motori, R. Cartoni, S.-K. Kwon, and J. Courchet, "Pleiotropic mitochondria: The influence of mitochondria on neuronal development and disease," *Journal of Neuroscience*, vol. 39, no. 42, pp. 8200–8208, 2019.

[6] G. Kroemer, L. Galluzzi, and C. Brenner, "Mitochondrial membrane permeabilization in cell death," *Physiological reviews*, vol. 87, no. 1, pp. 99–163, 2007.

[7] X. Saelens, N. Festjens, L. V. Walle, M. Van Gurp, G. van Loo, and P. Vandenabeele, "Toxic proteins released from mitochondria in cell death," *Oncogene*, vol. 23, no. 16, p. 2861, 2004.

[8] S. Cory and J. M. Adams, "The bcl2 family: regulators of the cellular life-or-death switch," *Nature Reviews Cancer*, vol. 2, no. 9, p. 647, 2002.

[9] B. N. Dugger and D. W. Dickson, "Pathology of neurodegenerative diseases," *Cold Spring Harbor perspectives in biology*, vol. 9, no. 7, p. a028035, 2017.

[10] M. Kritsilis, S. V Rizou, P. N. Koutsoudaki, K. Evangelou, V. G. Gorgoulis, and D. Papadopoulos, "Ageing, cellular senescence and neurodegenerative disease," *International journal of molecular sciences*, vol. 19, no. 10, p. 2937, 2018.

[11] V. Castelli, E. Benedetti, A. Antonosante, M. Catanesi, G. Pitari, R. Ippoliti, A. Cimini, and M. d'Angelo, "Neuronal cells rearrangement during aging and neurodegenerative disease: Metabolism, oxidative stress and organelles dynamic," *Frontiers in molecular neuroscience*, vol. 12, 2019.

[12] H. Kawamata and G. Manfredi, "Proteinopathies and oxphos dysfunction in neurodegenerative diseases," *J Cell Biol*, vol. 216, no. 12, pp. 3917–3929, 2017.

[13] E. Lévy, N. El Banna, D. Baïlle, A. Heneman-Masurel, S. Truchet, H. Rezaei, M.-E. Huang, V. Béringue, D. Martin, and L. Vernis, "Causative links between protein aggregation and oxidative stress: A review," *International journal of molecular sciences*, vol. 20, no. 16, p. 3896, 2019.

[14] M. Katsuno, K. Sahashi, Y. Iguchi, and A. Hashizume, "Preclinical progression of neurodegenerative diseases," *Nagoya journal of medical science*, vol. 80, no. 3, p. 289, 2018.

[15] M. P. Mattson and T. V. Arumugam, "Hallmarks of brain aging: adaptive and pathological modification by metabolic states," *Cell metabolism*, vol. 27, no. 6, pp. 1176–1199, 2018.

[16] C. López-Otín, L. Galluzzi, J. M. Freije, F. Madeo, and G. Kroemer, "Metabolic control of longevity," *Cell*, vol. 166, no. 4, pp. 802–821, 2016.

[17] Y. Zhou and N. Danbolt, "Glutamate as a neurotransmitter in the healthy brain," *Journal of neural transmission*, vol. 121, no. 8, pp. 799–817, 2014.

[18] D. W. Choi, "Glutamate neurotoxicity and diseases of the nervous system," *Neuron*, vol. 1, no. 8, pp. 623–634, 1988.

[19] T. H. Murphy, M. Miyamoto, A. Sastre, R. L. Schnaar, and J. T. Coyle, "Glutamate toxicity in a neuronal cell line involves inhibition of cystine transport leading to oxidative stress," *Neuron*, vol. 2, no. 6, pp. 1547–1558, 1989.

[20] S. Tan, D. Schubert, and P. Maher, "Oxytosis: a novel form of programmed cell death," *Current topics in medicinal chemistry*, vol. 1, no. 6, pp. 497–506, 2001.

[21] D. Schubert and D. Piasecki, "Oxidative glutamate toxicity can be a component of the excitotoxicity cascade," *Journal of Neuroscience*, vol. 21, no. 19, pp. 7455–7462, 2001.

[22] A. Oka, M. J. Belliveau, P. A. Rosenberg, and J. J. Volpe, "Vulnerability of oligodendroglia to glutamate: pharmacology, mechanisms, and prevention," *Journal of Neuroscience*, vol. 13, no. 4, pp. 1441–1453, 1993.

[23] S. Toppo, L. Flohé, F. Ursini, S. Vanin, and M. Maiorino, "Catalytic mechanisms and specificities of glutathione peroxidases: variations of a basic scheme," *Biochimica et Biophysica Acta (BBA)-General Subjects*, vol. 1790, no. 11, pp. 1486–1500, 2009.

[24] A. Seiler, M. Schneider, H. Förster, S. Roth, E. K. Wirth, C. Culmsee, N. Plesnila, E. Kremmer, O. Rådmark, W. Wurst *et al.*, "Glutathione peroxidase 4 senses and translates oxidative stress into 12/15-lipoxygenase dependent-and aif-mediated cell death," *Cell metabolism*, vol. 8, no. 3, pp. 237–248, 2008.

[25] C. Kubota, S. Torii, N. Hou, N. Saito, Y. Yoshimoto, H. Imai, and T. Takeuchi, "Constitutive reactive oxygen species generation from autophagosome/lysosome in neuronal oxidative toxicity," *Journal of Biological Chemistry*, vol. 285, no. 1, pp. 667–674, 2010.

[26] S. Doll, B. Proneth, Y. Y. Tyurina, E. Panzilius, S. Kobayashi, I. Ingold, M. Irmler, J. Beckers, M. Aichler, A. Walch *et al.*, "Acsl4 dictates ferroptosis sensitivity by shaping cellular lipid composition," *Nature chemical biology*, vol. 13, no. 1, p. 91, 2017.

[27] V. E. Kagan, G. Mao, F. Qu, J. P. F. Angeli, S. Doll, C. St Croix, H. H. Dar, B. Liu, V. A. Tyurin, V. B. Ritov *et al.*, "Oxidized arachidonic and adrenic pes navigate cells to ferroptosis," *Nature chemical biology*, vol. 13, no. 1, p. 81, 2017.

[28] S. E. Wenzel, Y. Y. Tyurina, J. Zhao, C. M. S. Croix, H. H. Dar, G. Mao, V. A. Tyurin, T. S. Anthonymuthu, A. A. Kapralov, A. A. Amoscato *et al.*, "Pebp1 wardens ferroptosis by enabling lipoxygenase generation of lipid death signals," *Cell*, vol. 171, no. 3, pp. 628–641, 2017.

[29] T. S. Anthonymuthu, E. M. Kenny, I. Shrivastava, Y. Y. Tyurina, Z. E. Hier, H.-C. Ting, H. H. Dar, V. A. Tyurin, A. Nesterova, A. A. Amoscato *et al.*, "Empowerment of 15-lipoxygenase catalytic competence in selective oxidation of membrane ete-pe to ferroptotic death signals, hpete-pe," *Journal of the American Chemical Society*, vol. 140, no. 51, pp. 17 835–17 839, 2018.

[30] R. Shah, M. S. Shchepinov, and D. A. Pratt, "Resolving the role of lipoxygenases in the initiation and execution of ferroptosis," *ACS central science*, vol. 4, no. 3, pp. 387–396, 2018.

[31] L. P. Shornick and M. Holtzman, "A cryptic, microsomal-type arachidonate 12-lipoxygenase is tonically inactivated by oxidation-reduction conditions in cultured epithelial cells." *Journal of Biological Chemistry*, vol. 268, no. 1, pp. 371–376, 1993.

[32] W. Hagmann, D. Kagawa, C. Renaud, and K. Honn, "Activity and protein distribution of 12-lipoxygenase in hel cells: induction of membrane-association by phorbol ester tpa, modulation of activity by glutathione and 13-hpode, and ca2+-dependent translocation to membranes," *Prostaglandins*, vol. 46, no. 6, pp. 471–477, 1993.

[33] Y. Li, P. Maher, and D. Schubert, "A role for 12-lipoxygenase in nerve cell death caused by glutathione depletion," *Neuron*, vol. 19, no. 2, pp. 453–463, 1997.

[34] S. Pallast, K. Arai, X. Wang, E. H. Lo, and K. Van Leyen, "12/15-lipoxygenase targets neuronal mitochondria under oxidative stress," *Journal of neurochemistry*, vol. 111, no. 3, pp. 882–889, 2009.

[35] N. Henke, P. Albrecht, I. Bouchachia, M. Ryazantseva, K. Knoll, J. Lewerenz, E. Kaznacheyeva, P. Maher, and A. Methner, "The plasma membrane channel orai1 mediates detrimental calcium influx caused by endogenous oxidative stress," *Cell death & disease*, vol. 4, no. 1, p. e470, 2013.

[36] N. Doti, C. Reuther, P. Scognamiglio, A. Dolga, N. Plesnila, M. Ruvo, and C. Culmsee, "Inhibition of the aif/cypa complex protects against intrinsic death pathways induced by oxidative stress," *Cell death & disease*, vol. 5, no. 1, p. e993, 2014.

[37] B. Honrath, I. Metz, N. Bendridi, J. Rieusset, C. Culmsee, and A. M. Dolga, "Glucose-regulated protein 75 determines er–mitochondrial coupling and sensitivity to oxidative stress in neuronal cells," *Cell death discovery*, vol. 3, p. 17076, 2017.

[38] P. Maher, K. van Leyen, P. N. Dey, B. Honrath, A. Dolga, and A. Methner, "The role of ca2+ in cell death caused by oxidative glutamate toxicity and ferroptosis," *Cell Calcium*, vol. 70, pp. 47–55, 2018.

[39] P. Nagakannan, M. I. Islam, S. Karimi-Abdolrezaee, and E. Eftekharpour, "Inhibition of vdac1 protects against glutamate-induced oxytosis and mitochondrial fragmentation in hippocampal ht22 cells," *Cellular and molecular neurobiology*, vol. 39, no. 1, pp. 73–85, 2019.

[40] S. Kumari, S. L. Mehta, and P. A. Li, "Glutamate induces mitochondrial dynamic imbalance and autophagy activation: preventive effects of selenium," *PloS one*, vol. 7, no. 6, p. e39382, 2012.

[41] J. Grohm, S. Kim, U. Mamrak, S. Tobaben, A. Cassidy-Stone, J. Nunnari, N. Plesnila, and C. Culmsee, "Inhibition of drp1 provides neuroprotection in vitro and in vivo," *Cell death and differentiation*, vol. 19, no. 9, p. 1446, 2012.

[42] S. Landshamer, M. Hoehn, N. Barth, S. Duvezin-Caubet, G. Schwake, S. Tobaben, I. Kazhdan, B. Becattini, S. Zahler, A. Vollmar *et al.*, "Bid-induced release of aif from mitochondria causes immediate neuronal cell death," *Cell death and differentiation*, vol. 15, no. 10, p. 1553, 2008.

[43] J. Grohm, N. Plesnila, and C. Culmsee, "Bid mediates fission, membrane permeabilization and peri-nuclear accumulation of mitochondria as a prerequisite for oxidative neuronal cell death," *Brain, behavior, and immunity*, vol. 24, no. 5, pp. 831–838, 2010.

[44] M. Zille, A. Kumar, N. Kundu, M. W. Bourassa, V. S. Wong, D. Willis, S. S. Karuppagounder, and R. R. Ratan, "Ferroptosis in neurons and cancer cells is similar but differentially regulated by histone deacetylase inhibitors," *eNeuro*, vol. 6, no. 1, 2019.

[45] M. Gao, P. Monian, N. Quadri, R. Ramasamy, and X. Jiang, "Glutaminolysis and transferrin regulate ferroptosis," *Molecular cell*, vol. 59, no. 2, pp. 298–308, 2015.

[46] H. Nishizawa, M. Matsumoto, T. Shindo, D. Saigusa, H. Kato, K. Suzuki, M. Sato, Y. Ishii, H. Shimokawa, and K. Igarashi, "Ferroptosis is controlled by the coordinated transcriptional regulation of glutathione and labile iron metabolism by the transcription factor bach1," *Journal of Biological Chemistry*, vol. 295, no. 1, pp. 69–82, 2020.

[47] S. A. Novgorodov, J. R. Voltin, M. A. Gooz, L. Li, J. J. Lemasters, and T. I. Gudz, "Acid sphingomyelinase promotes mitochondrial dysfunction due to glutamate-induced regulated necrosis," *Journal of lipid research*, vol. 59, no. 2, pp. 312–329, 2018.

[48] S. Doll, F. P. Freitas, R. Shah, M. Aldrovandi, M. C. da Silva, I. Ingold, A. G. Grocin, T. N. X. da Silva, E. Panzilius, C. Scheel *et al.*, "Fsp1 is a glutathione-independent ferroptosis suppressor," *Nature*, pp. 1–1, 2019.

[49] K. Bersuker, J. Hendricks, Z. Li, L. Magtanong, B. Ford, P. H. Tang, M. A. Roberts, B. Tong, T. J. Maimone, R. Zoncu *et al.*, "The coq oxidoreductase fsp1 acts parallel to gpx4 to inhibit ferroptosis," *Nature*, pp. 1–1, 2019.

[50] K. Shimada, M. Hayano, N. C. Pagano, and B. R. Stockwell, "Cell-line selectivity improves the predictive power of pharmacogenomic analyses and helps identify nadph as biomarker for ferroptosis sensitivity," *Cell chemical biology*, vol. 23, no. 2, pp. 225–235, 2016.

[51] S. Tan, Y. Sagara, Y. Liu, P. Maher, and D. Schubert, "The regulation of reactive oxygen species production during programmed cell death," *The Journal of cell biology*, vol. 141, no. 6, pp. 1423–1432, 1998.

[52] E.-M. Öxler, A. Dolga, and C. Culmsee, "Aif depletion provides neuroprotection through a preconditioning effect," *Apoptosis*, vol. 17, no. 10, pp. 1027–1038, 2012.

[53] P. Maher and J. B. Davis, "The role of monoamine metabolism in oxidative glutamate toxicity," *Journal of Neuroscience*, vol. 16, no. 20, pp. 6394–6401, 1996.

[54] A. Dolga, I. Krabbendam, B. Honrath, B. Dilberger, M. Schmidt, G. Eckert, and C. Culmsee, "Metabolic escape to glycolysis through sk channel activation inhibits ferroptosis and increases the life span of c. elegans in conditions of heat stress," *The FASEB Journal*, vol. 33, no. 1_supplement, pp. 665–7, 2019.

[55] A. M. Dolga, M. F. Netter, F. Perocchi, N. Doti, L. Meissner, S. Tobaben, J. Grohm, H. Zischka, N. Plesnila, N. Decher *et al.*, "Mitochondrial small conductance sk2 channels prevent glutamate-induced oxytosis and mitochondrial dysfunction," *Journal of Biological Chemistry*, vol. 288, no. 15, pp. 10 792–10 804, 2013.

[56] T. Xu, W. Ding, X. Ji, X. Ao, Y. Liu, W. Yu, and J. Wang, "Molecular mechanisms of ferroptosis and its role in cancer therapy," *Journal of cellular and molecular medicine*, 2019.

[57] A. Pfeiffer, M. Jaeckel, J. Lewerenz, R. Noack, A. Pouya, T. Schacht, C. Hoffmann, J. Winter, S. Schweiger, M. K. Schäfer *et al.*, "Mitochondrial function and energy metabolism in neuronal ht22 cells resistant to oxidative stress," *British journal of pharmacology*, vol. 171, no. 8, pp. 2147–2158, 2014.

[58] J. Lewerenz, G. Ates, A. Methner, M. Conrad, and P. Maher, "Oxytosis/ferroptosis—(re-) emerging roles for oxidative stress-dependent non-apoptotic cell death in diseases of the central nervous system," *Frontiers in Neuroscience*, vol. 12, 2018.

[59] B. Onken and M. Driscoll, "Metformin induces a dietary restriction–like state and the oxidative stress response to extend c. elegans healthspan via ampk, lkb1, and skn-1," *PloS one*, vol. 5, no. 1, p. e8758, 2010.

[60] N. Barzilai, J. P. Crandall, S. B. Kritchevsky, and M. A. Espeland, "Metformin as a tool to target aging," *Cell metabolism*, vol. 23, no. 6, pp. 1060–1065, 2016.

[61] E. Sanchez-Rangel and S. E. Inzucchi, "Metformin: clinical use in type 2 diabetes," *Diabetologia*, vol. 60, no. 9, pp. 1586–1593, 2017.

[62] S. El Messaoudi, G. A. Rongen, R. A. de Boer, and N. P. Riksen, "The cardioprotective effects of metformin," *Current opinion in lipidology*, vol. 22, no. 6, pp. 445–453, 2011.

[63] Z. Polianskyte-Prause, T. A. Tolvanen, S. Lindfors, V. Dumont, M. Van, H. Wang, S. N. Dash, M. Berg, J.-B. Naams, L. C. Hautala *et al.*, "Metformin increases glucose uptake and acts renoprotectively by reducing ship2 activity," *The FASEB Journal*, vol. 33, no. 2, pp. 2858–2869, 2018.

[64] A. Yerevanian and A. A. Soukas, "Metformin: Mechanisms in human obesity and weight loss," *Current obesity reports*, vol. 8, no. 2, pp. 156–164, 2019.

[65] I. Pradas, S. Rovira-Llopis, A. Naudí, C. Bañuls, M. Rocha, A. Hernandez-Mijares, R. Pamplona, V. M. Victor, and M. Jové, "Metformin induces lipid changes on sphingolipid species and oxidized lipids in polycystic ovary syndrome women," *Scientific reports*, vol. 9, no. 1, pp. 1–11, 2019.

[66] R. Romero, O. Erez, M. Hüttemann, E. Maymon, B. Panaitescu, A. Conde-Agudelo, P. Pacora, B. H. Yoon, and L. I. Grossman, "Metformin, the aspirin of the 21st century: its role in gestational diabetes mellitus, prevention of preeclampsia and cancer, and the promotion of longevity," *American journal of obstetrics and gynecology*, vol. 217, no. 3, pp. 282–302, 2017.

[67] C. J. Green, T. Marjot, J. W. Tomlinson, and L. Hodson, "Of mice and men: Is there a future for metformin in the treatment of hepatic steatosis?" *Diabetes, Obesity and Metabolism*, vol. 21, no. 4, pp. 749–760, 2019.

[68] J. Zhou, S. Massey, D. Story, and L. Li, "Metformin: an old drug with new applications," *International journal of molecular sciences*, vol. 19, no. 10, p. 2863, 2018.

[69] Q. Wang, M. Zhang, G. Torres, S. Wu, C. Ouyang, Z. Xie, and M.-H. Zou, "Metformin suppresses diabetes-accelerated atherosclerosis via the inhibition of drp1-mediated mitochondrial fission," *Diabetes*, vol. 66, no. 1, pp. 193–205, 2017.

[70] K. Chen, Z.-W. Lin, S.-m. He, C.-q. Wang, J.-c. Yang, Y. Lu, X.-b. Xie, and Q. Li, "Metformin inhibits the proliferation of rheumatoid arthritis fibroblast-like synoviocytes through igf-ir/pi3k/akt/m-tor pathway," *Biomedicine & Pharmacotherapy*, vol. 115, p. 108875, 2019.

[71] S. Safe, V. Nair, and K. Karki, "Metformin-induced anticancer activities: recent insights," *Biological chemistry*, vol. 399, no. 4, pp. 321–335, 2018.

[72] M. N. Pollak, "Investigating metformin for cancer prevention and treatment: the end of the beginning," *Cancer discovery*, vol. 2, no. 9, pp. 778–790, 2012.

[73] J. He, K. Wang, N. Zheng, Y. Qiu, G. Xie, M. Su, W. Jia, and H. Li, "Metformin suppressed the proliferation of lovo cells and induced a time-dependent metabolic and transcriptional alteration," *Scientific reports*, vol. 5, p. 17423, 2015.

[74] R. B. Grigolon, E. Brietzke, R. B. Mansur, M. Idzikowski, F. Gerchman, F. G. De Felice, and R. S. McIntyre, "Association between diabetes and mood disorders and the potential use of anti-hyperglycemic agents as antidepressants," *Progress in Neuro-Psychopharmacology and Biological Psychiatry*, p. 109720, 2019.

[75] C. Rotermund, G. Machetanz, and J. C. Fitzgerald, "The therapeutic potential of metformin in neurodegenerative diseases," *Frontiers in endocrinology*, vol. 9, 2018.

[76] K. Isoda, J. L. Young, A. Zirlik, L. A. MacFarlane, N. Tsuboi, N. Gerdes, U. Schonbeck, and P. Libby, "Metformin inhibits proinflammatory responses and nuclear factor-κb in human vascular wall cells," *Arteriosclerosis, thrombosis, and vascular biology*, vol. 26, no. 3, pp. 611–617, 2006.

[77] G. Tang, H. Yang, J. Chen, M. Shi, L. Ge, X. Ge, and G. Zhu, "Metformin ameliorates sepsis-induced brain injury by inhibiting apoptosis, oxidative stress and neuroinflammation via the pi3k/akt signaling pathway," *Oncotarget*, vol. 8, no. 58, p. 97977, 2017.

[78] Q. Chen, J. Thompson, Y. Hu, A. Das, and E. J. Lesnefsky, "Metformin attenuates er stress–induced mitochondrial dysfunction," *Translational Research*, vol. 190, pp. 40–50, 2017.

[79] J. Ye, D. Luo, X. Xu, M. Sun, X. Su, Z. Tian, M. Zhang, C. Yu, and Q. Guan, "Metformin improves fertility in obese males by alleviating oxidative stress-induced blood-testis barrier damage," *Oxidative medicine and cellular longevity*, vol. 2019, 2019.

[80] M. D. Fullerton, S. Galic, K. Marcinko, S. Sikkema, T. Pulinilkunnil, Z.-P. Chen, H. M. O'neill, R. J. Ford, R. Palanivel, M. O'brien *et al.*, "Single phosphorylation sites in acc1 and acc2 regulate lipid homeostasis and the insulin-sensitizing effects of metformin," *Nature medicine*, vol. 19, no. 12, p. 1649, 2013.

[81] C. A. Collier, C. R. Bruce, A. C. Smith, G. Lopaschuk, and D. J. Dyck, "Metformin counters the insulin-induced suppression of fatty acid oxidation and stimulation of triacylglycerol storage in rodent skeletal muscle," *American Journal of Physiology-Endocrinology and Metabolism*, vol. 291, no. 1, pp. E182–E189, 2006.

[82] M.-Y. El-Mir, V. Nogueira, E. Fontaine, N. Avéret, M. Rigoulet, and X. Leverve, "Dimethylbiguanide inhibits cell respiration via an indirect effect targeted on the respiratory chain complex i," *Journal of Biological Chemistry*, vol. 275, no. 1, pp. 223–228, 2000.

[83] E. DORAN, A. P. HALESTRAP *et al.*, "Evidence that metformin exerts its anti-diabetic effects through inhibition of complex 1 of the mitochondrial respiratory chain," *Biochemical Journal*, vol. 348, no. 3, pp. 607–614, 2000.

[84] W.-L. Hou, J. Yin, M. Alimujiang, X.-Y. Yu, L.-G. Ai, Y.-q. Bao, F. Liu, and W.-P. Jia, "Inhibition of mitochondrial complex i improves glucose metabolism independently of ampk activation," *Journal of cellular and molecular medicine*, vol. 22, no. 2, pp. 1316–1328, 2018.

[85] L. Yang, H. Sha, R. L. Davisson, and L. Qi, "Phenformin activates the unfolded protein response in an amp-activated protein kinase (ampk)-dependent manner," *Journal of Biological Chemistry*, vol. 288, no. 19, pp. 13 631–13 638, 2013.

[86] A. Kalender, A. Selvaraj, S. Y. Kim, P. Gulati, S. Brûlé, B. Viollet, B. E. Kemp, N. Bardeesy, P. Dennis, J. J. Schlager *et al.*, "Metformin, independent of ampk, inhibits mtorc1 in a rag gtpase-dependent manner," *Cell metabolism*, vol. 11, no. 5, pp. 390–401, 2010.

[87] D. G. Hardie, F. A. Ross, and S. A. Hawley, "Ampk: a nutrient and energy sensor that maintains energy homeostasis," *Nature reviews Molecular cell biology*, vol. 13, no. 4, p. 251, 2012.

[88] D. G. Hardie, "Ampk—sensing energy while talking to other signaling pathways," *Cell metabolism*, vol. 20, no. 6, pp. 939–952, 2014.

[89] D. Garcia and R. J. Shaw, "Ampk: mechanisms of cellular energy sensing and restoration of metabolic balance," *Molecular cell*, vol. 66, no. 6, pp. 789–800, 2017.

[90] C. Cantó, Z. Gerhart-Hines, J. N. Feige, M. Lagouge, L. Noriega, J. C. Milne, P. J. Elliott, P. Puigserver, and J. Auwerx, "Ampk regulates energy expenditure by modulating nad+ metabolism and sirt1 activity," *Nature*, vol. 458, no. 7241, p. 1056, 2009.

[91] J. Kim, M. Kundu, B. Viollet, and K.-L. Guan, "Ampk and mtor regulate autophagy through direct phosphorylation of ulk1," *Nature cell biology*, vol. 13, no. 2, p. 132, 2011.

[92] M. Jang, R. Park, H. Kim, S. Namkoong, D. Jo, Y. H. Huh, I.-S. Jang, J. I. Lee, and J. Park, "Ampk contributes to autophagosome maturation and lysosomal fusion," *Scientific reports*, vol. 8, no. 1, p. 12637, 2018.

[93] K. Burkewitz, Y. Zhang, and W. B. Mair, "Ampk at the nexus of energetics and aging," *Cell metabolism*, vol. 20, no. 1, pp. 10–25, 2014.

[94] T. L. Marin, B. Gongol, F. Zhang, M. Martin, D. A. Johnson, H. Xiao, Y. Wang, S. Subramaniam, S. Chien, and J. Y.-J. Shyy, "Ampk promotes mitochondrial biogenesis and function by phosphorylating the epigenetic factors dnmt1, rbbp7, and hat1," *Sci. Signal.*, vol. 10, no. 464, p. eaaf7478, 2017.

[95] H. Zong, J. M. Ren, L. H. Young, M. Pypaert, J. Mu, M. J. Birnbaum, and G. I. Shulman, "Amp kinase is required for mitochondrial biogenesis in skeletal muscle in response to chronic energy deprivation," *Proceedings of the national academy of sciences*, vol. 99, no. 25, pp. 15 983–15 987, 2002.

[96] C. Settembre, R. Zoncu, D. L. Medina, F. Vetrini, S. Erdin, S. Erdin, T. Huynh, M. Ferron, G. Karsenty, M. C. Vellard *et al.*, "A lysosome-to-nucleus signalling mechanism senses and regulates the lysosome via mtor and tfeb," *The EMBO journal*, vol. 31, no. 5, pp. 1095–1108, 2012.

[97] A. Bartolomé, A. García-Aguilar, S.-I. Asahara, Y. Kido, C. Guillén, U. B. Pajvani, and M. Benito, "Mtorc1 regulates both general autophagy and mitophagy induction after oxidative phosphorylation uncoupling," *Molecular and cellular biology*, vol. 37, no. 23, pp. e00 441–17, 2017.

[98] D. Ebrahimi-Fakhari, A. Saffari, L. Wahlster, A. Di Nardo, D. Turner, T. L. Lewis Jr, C. Conrad, J. M. Rothberg, J. O. Lipton, S. Kölker *et al.*, "Impaired mitochondrial dynamics and mitophagy in neuronal models of tuberous sclerosis complex," *Cell reports*, vol. 17, no. 4, pp. 1053–1070, 2016.

[99] D. W. Lamming, "Inhibition of the mechanistic target of rapamycin (mtor)–rapamycin and beyond," *Cold Spring Harbor perspectives in medicine*, vol. 6, no. 5, p. a025924, 2016.

[100] D. E. Harrison, R. Strong, Z. D. Sharp, J. F. Nelson, C. M. Astle, K. Flurkey, N. L. Nadon, J. E. Wilkinson, K. Frenkel, C. S. Carter *et al.*, "Rapamycin fed late in life extends lifespan in genetically heterogeneous mice," *nature*, vol. 460, no. 7253, p. 392, 2009.

[101] A. Martin-Montalvo, E. M. Mercken, S. J. Mitchell, H. H. Palacios, P. L. Mote, M. Scheibye-Knudsen, A. P. Gomes, T. M. Ward, R. K. Minor, M.-J. Blouin *et al.*, "Metformin improves healthspan and lifespan in mice," *Nature communications*, vol. 4, p. 2192, 2013.

[102] V. N. Anisimov, A. V. Semenchenko, and A. I. Yashin, "Insulin and longevity: antidiabetic biguanides as geroprotectors," *Biogerontology*, vol. 4, no. 5, pp. 297–307, 2003.

[103] Y. Shitara, N. Nakamichi, M. Norioka, H. Shima, Y. Kato, and T. Horie, "Role of organic cation/carnitine transporter 1 in uptake of phenformin and inhibitory effect on complex i respiration in mitochondria," *toxicological sciences*, vol. 132, no. 1, pp. 32–42, 2012.

[104] C. R. Sirtori and C. Pasik, "Re-evaluation of a biguanide, metformin: mechanism of action and tolerability," *Pharmacological research*, vol. 30, no. 3, pp. 187–228, 1994.

[105] A. R. Cameron, L. Logie, K. Patel, S. Erhardt, S. Bacon, P. Middleton, J. Harthill, C. Forteath, J. T. Coats, C. Kerr *et al.*, "Metformin selectively targets redox control of complex i energy transduction," *Redox biology*, vol. 14, pp. 187–197, 2018.

[106] O. Jalling and C. Olsen, "The effects of metformin compared to the effects of phenformin on the lactate production and the metabolism of isolated parenchymal rat liver cell." *Acta pharmacologica et toxicologica*, vol. 54, no. 5, pp. 327–332, 1984.

[107] E. D. Segal, A. Yasmeen, M.-C. Beauchamp, J. Rosenblatt, M. Pollak, and W. H. Gotlieb, "Relevance of the oct1 transporter to the antineoplastic effect of biguanides," *Biochemical and biophysical research communications*, vol. 414, no. 4, pp. 694–699, 2011.

[108] D.-S. Wang, J. W. Jonker, Y. Kato, H. Kusuhara, A. H. Schinkel, and Y. Sugiyama, "Involvement of organic cation transporter 1 in hepatic and intestinal distribution of metformin," *Journal of Pharmacology and Experimental Therapeutics*, vol. 302, no. 2, pp. 510–515, 2002.

[109] H. R. Bridges, A. J. Jones, M. N. Pollak, and J. Hirst, "Effects of metformin and other biguanides on oxidative phosphorylation in mitochondria," *Biochemical Journal*, vol. 462, no. 3, pp. 475–487, 2014.

[110] S. Heinz, A. Freyberger, B. Lawrenz, L. Schladt, G. Schmuck, and H. Ellinger-Ziegelbauer, "Energy metabolism modulation by biguanides in comparison with rotenone in rat liver and heart," *Archives of toxicology*, pp. 1–13, 2019.

[111] L. Logie, J. Harthill, K. Patel, S. Bacon, D. L. Hamilton, K. Macrae, G. McDougall, H.-H. Wang, L. Xue, H. Jiang *et al.*, "Cellular responses to the metal-binding properties of metformin," *Diabetes*, vol. 61, no. 6, pp. 1423–1433, 2012.

[112] Z. Drahota, E. Palenickova, R. Endlicher, M. Milerova, J. Brejchova, M. Vosahlikova, P. Svoboda, L. Kazdova, M. Kalous, Z. Cervinkova *et al.*, "Biguanides inhibit complex i, ii and iv of rat liver mitochondria and modify their functional properties." *Physiological research*, vol. 63, no. 1, 2014.

[113] G. Schäfer, "Site-specific uncoupling and inhibition of oxidative phosphorylation by biguanides. ii," *Biochimica et Biophysica Acta (BBA)-Bioenergetics*, vol. 172, no. 2, pp. 334–337, 1969.

[114] R. Fato, C. Bergamini, M. Bortolus, A. L. Maniero, S. Leoni, T. Ohnishi, and G. Lenaz, "Differential effects of mitochondrial complex i inhibitors on production

of reactive oxygen species," *Biochimica et Biophysica Acta (BBA)-Bioenergetics*, vol. 1787, no. 5, pp. 384–392, 2009.

[115] W. De Haes, L. Frooninckx, R. Van Assche, A. Smolders, G. Depuydt, J. Billen, B. P. Braeckman, L. Schoofs, and L. Temmerman, "Metformin promotes lifespan through mitohormesis via the peroxiredoxin prdx-2," *Proceedings of the National Academy of Sciences*, vol. 111, no. 24, pp. E2501–E2509, 2014.

[116] C. Batandier, B. Guigas, D. Detaille, M. El-Mir, E. Fontaine, M. Rigoulet, and X. M. Leverve, "The ros production induced by a reverse-electron flux at respiratory-chain complex 1 is hampered by metformin," *Journal of bioenergetics and biomembranes*, vol. 38, no. 1, pp. 33–42, 2006.

[117] C. Algire, O. Moiseeva, X. Deschênes-Simard, L. Amrein, L. Petruccelli, E. Birman, B. Viollet, G. Ferbeyre, and M. N. Pollak, "Metformin reduces endogenous reactive oxygen species and associated dna damage," *Cancer Prevention Research*, vol. 5, no. 4, pp. 536–543, 2012.

[118] H. Khan, A. Anshu, A. Prasad, S. Roy, J. Jeffery, W. Kittipongdaja, D. T. Yang, and S. M. Schieke, "Metabolic rewiring in response to biguanides is mediated by mros/hif-1a in malignant lymphocytes," *Cell Reports*, vol. 29, no. 10, pp. 3009–3018, 2019.

[119] S. Matsuzaki and K. M. Humphries, "Selective inhibition of deactivated mitochondrial complex i by biguanides," *Biochemistry*, vol. 54, no. 11, pp. 2011–2021, 2015.

[120] K. R. Pryde and J. Hirst, "Superoxide is produced by the reduced flavin in mitochondrial complex ia single, unified mechanism that applies during both forward and reverse electron transfer," *Journal of Biological Chemistry*, vol. 286, no. 20, pp. 18 056–18 065, 2011.

[121] L. Zhang, H. He, and J. A. Balschi, "Metformin and phenformin activate amp-activated protein kinase in the heart by increasing cytosolic amp concentration," *American Journal of Physiology-Heart and Circulatory Physiology*, vol. 293, no. 1, pp. H457–H466, 2007.

[122] Y.-L. Zhang, H. Guo, C.-S. Zhang, S.-Y. Lin, Z. Yin, Y. Peng, H. Luo, Y. Shi, G. Lian, C. Zhang *et al.*, "Amp as a low-energy charge signal autonomously initiates assembly of axin-ampk-lkb1 complex for ampk activation," *Cell metabolism*, vol. 18, no. 4, pp. 546–555, 2013.

[123] C.-S. Zhang, B. Jiang, M. Li, M. Zhu, Y. Peng, Y.-L. Zhang, Y.-Q. Wu, T. Y. Li, Y. Liang, Z. Lu *et al.*, "The lysosomal v-atpase-ragulator complex is a common activator for ampk and mtorc1, acting as a switch between catabolism and anabolism," *Cell metabolism*, vol. 20, no. 3, pp. 526–540, 2014.

[124] S. Meng, J. Cao, Q. He, L. Xiong, E. Chang, S. Radovick, F. E. Wondisford, and L. He, "Metformin activates amp-activated protein kinase by promoting formation of the $\alpha\beta\gamma$ heterotrimeric complex," *Journal of Biological Chemistry*, vol. 290, no. 6, pp. 3793–3802, 2015.

[125] Z. E. Gillespie, J. Pickering, and C. H. Eskiw, "Better living through chemistry: caloric restriction (cr) and cr mimetics alter genome function to promote increased health and lifespan," *Frontiers in genetics*, vol. 7, p. 142, 2016.

[126] B. Guigas, D. Detaille, C. Chauvin, C. Batandier, F. De Oliveira, E. Fontaine, and X. Leverve, "Metformin inhibits mitochondrial permeability transition and cell death: a pharmacological in vitro study," *Biochemical journal*, vol. 382, no. 3, pp. 877–884, 2004.

[127] M.-Y. El-Mir, D. Detaille, R. Gloria, M. Delgado-Esteban, B. Guigas, S. Attia, E. Fontaine, A. Almeida, X. Leverve *et al.*, "Neuroprotective role of antidiabetic drug metformin against apoptotic cell death in primary cortical neurons," *Journal of Molecular Neuroscience*, vol. 34, no. 1, pp. 77–87, 2008.

[128] E. Fontaine, "Metformin-induced mitochondrial complex i inhibition: Facts, uncertainties, and consequences," *Frontiers in endocrinology*, vol. 9, 2018.

[129] S. Müller, A. Versini, F. Sindikubwabo, G. Belthier, S. Niyomchon, J. Pannequin, L. Grimaud, T. Cañeque, and R. Rodriguez, "Metformin reveals a mitochondrial copper addiction of mesenchymal cancer cells," *PloS one*, vol. 13, no. 11, p. e0206764, 2018.

[130] L. Gan, M. Guo, J. Si, J. Zhang, Z. Liu, J. Zhao, F. Wang, J. Yan, H. Li, and H. Zhang, "Protective effects of phenformin on zebrafish embryonic neurodevelopmental toxicity induced by x-ray radiation," *Artificial cells, nanomedicine, and biotechnology*, vol. 47, no. 1, pp. 4202–4210, 2019.

[131] S. D. Gettings, J. E. Reeve, and L. J. King, "Possible role of intracellular ca2+ in the toxicity of phenformin," *Biochemical pharmacology*, vol. 37, no. 2, pp. 281–289, 1988.

[132] J. Lee, S. L. Chan, C. Lu, M. A. Lane, and M. P. Mattson, "Phenformin suppresses calcium responses to glutamate and protects hippocampal neurons against excitotoxicity," *Experimental neurology*, vol. 175, no. 1, pp. 161–167, 2002.

[133] N. B. Madungwe, N. F. Zilberstein, Y. Feng, and J. C. Bopassa, "Critical role of mitochondrial ros is dependent on their site of production on the electron transport chain in ischemic heart," *American journal of cardiovascular disease*, vol. 6, no. 3, p. 93, 2016.

[134] B. R. Stockwell, J. P. F. Angeli, H. Bayir, A. I. Bush, M. Conrad, S. J. Dixon, S. Fulda, S. Gascón, S. K. Hatzios, V. E. Kagan *et al.*, "Ferroptosis: a regulated cell death nexus linking metabolism, redox biology, and disease," *Cell*, vol. 171, no. 2, pp. 273–285, 2017.

[135] S. K. Bardaweel, H. A. Alsalamat, S. M. Aleidi, and R. M. Bashatwah, "Glucose deprivation enhances the antiproliferative effects of oral hypoglycemic biguanides in different molecular subtypes of breast cancer: An in vitro study," *Acta Pharmaceutica*, vol. 68, no. 4, pp. 517–524, 2018.

[136] J. Lewerenz, S. J. Hewett, Y. Huang, M. Lambros, P. W. Gout, P. W. Kalivas, A. Massie, I. Smolders, A. Methner, M. Pergande *et al.*, "The cystine/glutamate antiporter system xc- in health and disease: from molecular mechanisms to novel therapeutic opportunities," *Antioxidants & redox signaling*, vol. 18, no. 5, pp. 522–555, 2013.

[137] C. T. Hong, K.-Y. Chau, and A. H. Schapira, "Meclizine-induced enhanced glycolysis is neuroprotective in parkinson disease cell models," *Scientific reports*, vol. 6, p. 25344, 2016.

[138] K. A. Brand and U. Hermfisse, "Aerobic glycolysis by proliferating cells: a protective strategy against reactive oxygen species." *The FASEB journal*, vol. 11, no. 5, pp. 388–395, 1997.

[139] S.-B. Wu and Y.-H. Wei, "Ampk-mediated increase of glycolysis as an adaptive response to oxidative stress in human cells: implication of the cell survival in mitochondrial diseases," *Biochimica et Biophysica Acta (BBA)-Molecular Basis of Disease*, vol. 1822, no. 2, pp. 233–247, 2012.

[140] A. Dlasková, L. Hlavatá, and P. Ježek, "Oxidative stress caused by blocking of mitochondrial complex i h+ pumping as a link in aging/disease vicious cycle," *The international journal of biochemistry & cell biology*, vol. 40, no. 9, pp. 1792–1805, 2008.

[141] R. Akki, R. Siracusa, M. Cordaro, A. Remigante, R. Morabito, M. Errami, and A. Marino, "Adaptation to oxidative stress at cellular and tissue level," *Archives of Physiology and Biochemistry*, pp. 1–11, 2019.

[142] A. U. H. Khan, N. Allende-Vega, D. Gitenay, J. Garaude, D.-N. Vo, S. Belkhala, S. Gerbal-Chaloin, C. Gondeau, M. Daujat-Chavanieu, C. Delettre *et al.*, "Mitochondrial complex i activity signals antioxidant response through erk5," *Scientific reports*, vol. 8, no. 1, p. 7420, 2018.

[143] L. Bleier, I. Wittig, H. Heide, M. Steger, U. Brandt, and S. Droese, "Generator-specific targets of mitochondrial reactive oxygen species," *Free Radical Biology and Medicine*, vol. 78, pp. 1–10, 2015.

[144] P. S. Brookes, Y. Yoon, J. L. Robotham, M. Anders, and S.-S. Sheu, "Calcium, atp, and ros: a mitochondrial love-hate triangle," *American Journal of Physiology-Cell Physiology*, vol. 287, no. 4, pp. C817–C833, 2004.

[145] J. R. Koenitzer, G. Bonacci, S. R. Woodcock, C.-S. Chen, N. Cantu-Medellin, E. E. Kelley, and F. J. Schopfer, "Fatty acid nitroalkenes induce resistance to ischemic cardiac injury by modulating mitochondrial respiration at complex ii," *Redox biology*, vol. 8, pp. 1–10, 2016.

[146] G. Ashabi, L. Khalaj, F. Khodagholi, M. Goudarzvand, and A. Sarkaki, "Pre-treatment with metformin activates nrf2 antioxidant pathways and inhibits inflammatory responses through induction of ampk after transient global cerebral ischemia," *Metabolic brain disease*, vol. 30, no. 3, pp. 747–754, 2015.

[147] M. J. Kerins and A. Ooi, "The roles of nrf2 in modulating cellular iron homeostasis," *Antioxidants & redox signaling*, vol. 29, no. 17, pp. 1756–1773, 2018.

[148] H. Huang, M. Zhou, L. Ruan, D. Wang, H. Lu, J. Zhang, J. Chen, Y. Hu, and Z. Chai, "Ampk mediates the neurotoxicity of iron oxide nanoparticles retained in mitochondria or lysosomes," *Metallomics*, 2019.

[149] L. Núñez, R. A. Valero, L. Senovilla, S. Sanz-Blasco, J. García-Sancho, and C. Villalobos, "Cell proliferation depends on mitochondrial ca2+ uptake: inhibition by salicylate," *The Journal of physiology*, vol. 571, no. 1, pp. 57–73, 2006.

[150] T. Storozhevykh, Y. E. Senilova, T. Brustovetsky, V. Pinelis, and N. Brustovetsky, "Neuroprotective effect of kb-r7943 against glutamate excitotoxicity is related to mild mitochondrial depolarization," *Neurochemical research*, vol. 35, no. 2, pp. 323–335, 2010.

[151] J.-J. Wu, Y. Cui, Y.-S. Yang, S.-C. Jung, J. W. Hyun, Y.-H. Maeng, D.-B. Park, S.-R. Lee, S.-J. Kim, and S.-Y. Eun, "Mild mitochondrial depolarization is involved in a neuroprotective mechanism of citrus sunki peel extract," *Phytotherapy Research*, vol. 27, no. 4, pp. 564–571, 2013.

[152] R. A. Valero, L. Senovilla, L. Núñez, and C. Villalobos, "The role of mitochondrial potential in control of calcium signals involved in cell proliferation," *Cell calcium*, vol. 44, no. 3, pp. 259–269, 2008.

[153] R. J. Mailloux and M.-E. Harper, "Uncoupling proteins and the control of mitochondrial reactive oxygen species production," *Free Radical Biology and Medicine*, vol. 51, no. 6, pp. 1106–1115, 2011.

[154] S. Miwa, J. St-Pierre, L. Partridge, and M. D. Brand, "Superoxide and hydrogen peroxide production by drosophila mitochondria," *Free Radical Biology and Medicine*, vol. 35, no. 8, pp. 938–948, 2003.

[155] S. Andrzejewski, S.-P. Gravel, J. St-Pierre, and M. N. Pollak, "Dual mode of action of metformin on mitochondrial metabolism," *Cancer & metabolism*, vol. 2, no. S1, p. P4, 2014.

[156] K. Klöditz and B. Fadeel, "Three cell deaths and a funeral: macrophage clearance of cells undergoing distinct modes of cell death," *Cell death discovery*, vol. 5, no. 1, p. 65, 2019.

[157] W. S. Yang and B. R. Stockwell, "Synthetic lethal screening identifies compounds activating iron-dependent, nonapoptotic cell death in oncogenic-ras-harboring cancer cells," *Chemistry & biology*, vol. 15, no. 3, pp. 234–245, 2008.

[158] E. N. Maldonado, K. L. Sheldon, D. N. DeHart, J. Patnaik, Y. Manevich, D. M. Townsend, S. M. Bezrukov, T. K. Rostovtseva, and J. J. Lemasters, "Voltage-dependent anion channels modulate mitochondrial metabolism in cancer cells regulation by free tubulin and erastin," *Journal of Biological Chemistry*, vol. 288, no. 17, pp. 11 920–11 929, 2013.

List of Figures

List of Tables